Some Results from a Time-Dependent Thermodynamic Model of Sea Ice[1]

GARY A. MAYKUT AND NORBERT UNTERSTEINER

Department of Atmospheric Sciences and Geophysics Program
University of Washington, Seattle 98105

A one-dimensional thermodynamic model of sea ice is presented that includes the effects of snow cover, ice salinity, and internal heating due to penetration of solar radiation. Surface-energy balances determine rates of ablation and accretion; diffusion equations govern heat transport within the ice and snow. The incoming radiative and turbulent fluxes, oceanic heat flux, ice salinity, snow accumulation, and surface albedo are specified as functions of time. Starting from an arbitrary initial condition, the model is integrated numerically until annual equilibrium patterns of temperature and thickness are achieved. The model is applied to the central Arctic. Input values for the initial test of the model are based on observational data. Values predicted by the model for the average ice thickness (288 cm), amount of surface ablation (40 cm), and the temperature field all agree closely with field observations. Other results from the model indicate that, under present conditions, the ocean must supply 1 to 2 kcal/cm^2 year to the ice; an additional 4 kcal/cm^2 year would cause the ice to vanish. Annual snow depths less than 70 cm are shown to have little effect on equilibrium thickness; snow depths greater than 70 cm would result in much thicker ice. Comparison of observed and calculated temperature profiles suggest that about 2.0 to 2.5 kcal/cm^2 year of the incoming short-wave radiation penetrates the ice and contributes to internal heating. Average ice albedos under 0.50 would cause the ice to vanish in a few years.

Sea ice accounts (in areal extent) for nearly two-thirds of the earth's ice cover. Unlike the polar icecaps and alpine glaciers, its vertical dimension is small compared to its horizontal extent. In the Arctic, ice thickness averages 2–4 meters [*Lyon*, 1961; *Wittmann and Schule*, 1966]; however, there is a continuous frequency distribution from only a few centimeters for young ice to several tens of meters for pressure ice. Relatively minor changes in climate can thus produce large changes in the areal extent of the ice cover, significantly affecting the large-scale transfer of energy between the atmosphere and oceans. In some circumstances this might result in a positive feedback process that could continue to magnify the original change. Such considerations have led numerous investigators to look to the polar regions for a source of climatic changes associated with the ice ages of the Quaternary [*Brooks*, 1949; *Ewing and Donn*, 1956, 1958; *Donn and Ewing*, 1966; *Budyko*, 1966; *Fletcher*, 1969].

[1] Contribution 236, Department of Atmospheric Sciences, University of Washington, Seattle.

There is little doubt that there is an intimate connection between the state of the ice pack and hemispheric weather patterns, but it must be remembered that the atmosphere, oceans, and ice cover are all components of a single thermodynamic system, and a change in any one part necessarily results in compensating changes in the others. Separation of cause and effect is a necessary prerequisite to understanding the system. Although the physical principles governing the operation of each component are relatively well understood, complete solution of such a system is now beyond the range of our abilities.

Efforts to numerically simulate the behavior of the atmosphere have been highly successful. Even though the simulations do not completely describe atmospheric and oceanic interactions, short and medium-range forecasts have proven accurate because the major variations in the oceans proceed about 2 orders of magnitude more slowly than in the atmosphere. Comparable models of the oceans are being developed [e.g., *Bryan and Cox*, 1968]. Recently, *Manabe and Bryan* [1969] have reported initial results from a model which successfully couples the

ocean and atmosphere. In the polar oceans, however, a third medium, ice, adds further complexity to the system. Knowledge regarding its dynamic and thermodynamic behavior is therefore essential to the development of a comprehensive model.

Numerous attempts have been made to develop empirical relationships predicting ice growth from observed temperatures at the surface. Two of the best known of these are due to *Barnes* [1928] and *Zubov* [1943]. Somewhat more complex equations have been developed by *Bilello* [1961, 1964] from long-term observations of ice growth in the Arctic. Although empirical and statistical approaches have practical value, they offer little physical insight into the problem.

Since the classical work of *Stefan* [1891], theoretical studies of the rate of ice growth have generally been limited to those in which approximate analytical solutions could be obtained [*Kolesnikov*, 1946; *Doronin*, 1959, 1966b]. Analog circuits have also been designed to describe the growth of sea ice [*Schwerdtfeger*, 1964; *U. S. Naval Civil Engineering Laboratory*, 1965], but they are severely restricted in the sophistication of boundary conditions that may be employed. With the development of high-speed computers it is no longer necessary to find analytical solutions, as a system of integro-differential equations can be rapidly solved by finite-difference techniques. An advanced model of sea ice has been developed by *Budyko* [1966], who reports calculations of ice thickness and the horizontal extent of the ice pack in good agreement with observational evidence. The principal criticism of the Budyko model is that its upper boundary condition is more or less independent of heat conduction within the ice. By specifying surface temperatures, he ignores any effects of heat conduction on surface ablation and surface temperature. No provisions are made to account for snow cover or for the effects of ice salinity on heat transport between the boundaries of the slab. The model described by *Untersteiner* [1966] does not have these limitations.

DESCRIPTION OF THE MODEL

Ideally viewed, sea ice is an infinite horizontally homogeneous slab floating on its own liquid phase and having various energy fluxes impinging at both surfaces. The ice transfo heat between ocean and atmosphere by co duction; however, the transfer is affected by t brine pockets in the ice and by short-wa radiation penetrating the upper surface duri certain seasons. The annual snow cover i fluences the radiative and conductive transf in important ways and must be considered b addition of an appropriate second layer to t model. An internal boundary condition ties t gether the diffusion equations describing condu tion of heat in the snow and in the ice.

The boundaries of the slab are mathematical idealized planes. Energy is assumed to be a sorbed at these planes, although in reality th energy absorption occurs in a layer of fini thickness. Mass changes may occur at either th upper or lower surface. At the upper boundar ice or snow may melt, but mass may be i creased only through the addition of snow Either ablation or accretion can take place the bottom of the slab. The crux of the presen problem is the description of these mass change They are expressed by heat-balance equation that relate the various energy fluxes toward an away from the surfaces to the rates of freezin or melting.

At the upper boundary the major energ fluxes include incoming long-wave radiatio from the atmosphere and clouds (F_a), incomin solar short-wave radiation (F_s), reflected shor wave radiation (αF_s), and outgoing long-wa radiation ($\epsilon_s \sigma T_s^4$), where α is the surface albed ϵ_s is the long-wave emissivity, and σ is th Stefan-Boltzmann constant. In addition, the are several smaller but important fluxes: th fluxes of sensible heat (F_c) and latent heat (F_e in the adjacent air, heat conduction flux in th ice or snow (F_c), and a flux of radiative energ through the surface into the ice (I_0). The fluxes are schematically illustrated in Figure In describing the energy fluxes, the conventio that a flux toward the surface is positive an one away from the surface is negative will adopted.

To determine a balance equation for the upp boundary, it is necessary to consider two possibl situations. If the surface temperature (T_s) below the freezing point, T_f, must be adjust to balance all the fluxes. If, on the other han T_s is at the melting point, a certain amount ice will have to melt to accommodate any su

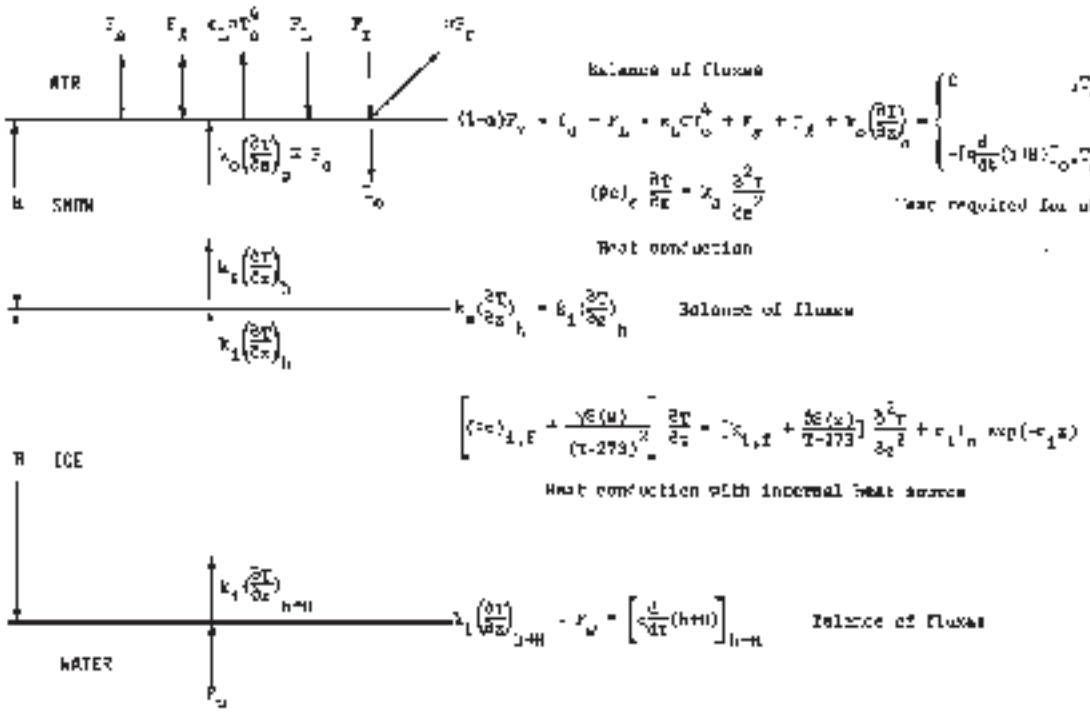

Fig. 1. Schematic illustration of the sea ice model.

plus of energy flux toward the surface

$$(1-\alpha)F_s - I_0 + F_L - \epsilon_L\sigma T_0^4 + F_s + F_l + k\left(\frac{\partial T}{\partial z}\right)_0 = 0 \text{ if } T_0 < 273^\circ\text{K} \qquad (1)$$

or

$$= -\left[\rho\frac{d}{dt}(h+H)\right]_0 \text{ if } T_0 = 273^\circ\text{K}$$

where h is the thickness of the snow layer, H is the thickness of the ice layer, and q is the latent heat of fusion of the surface material. The subscript 0 refers to the upper surface. I_0 is contained in $(1-\alpha)F_s$; however, since I_0 passes into the interior of the ice, it represents an energy loss by the surface and must be subtracted from the net short-wave radiation. The turbulent fluxes are given as positive terms, but they may in fact have either direction. The quantities in (1) that must be specified as time-dependent external parameters are α, F_s, F_L, I_0, F_l, and F_s; all temperatures and ice-thickness changes result from integration of the model. Snow deposition must also be treated as an external parameter.

The conduction of heat between the boundaries of the slab is complicated by the penetration and absorption of short-wave radiation creating internal heat sources that must be considered. During the snow-free summer months, for example, solar radiation penetrating the ice surface (I_0) is the prime source of internal heating. Because absorption of solar energy by the ice or snow is a function of wavelength, angle of incidence, and physical characteristics of the material, a theoretical description of I_0 would be complex. For modeling purposes, we may consider the ice slab to have two layers: a thin surface layer that absorbs most of the short-wave energy, overlying another layer in which the remaining energy is absorbed. Numerical limitations restrict the resolution of the model to the point that absorption of radiation in the surface layer is indistinguishable from direct surface melting. Observations by *Untersteiner* [1961] and *Cherepanov* [1966] indicate that, to a first approximation, extinction in the lower layer follows Beer's Law. If we then define a bulk (integrated over all wavelengths and solar angles) extinction coefficient (κ_i) and assume that the thermal conductivity (k_i) is constant, transfer of heat in the snow is described by

$$(\rho c)_s \frac{\partial T}{\partial t} = k_s \frac{\partial^2 T}{\partial z^2} + \kappa_s I_0 \exp(-\kappa_s z) \qquad (2)$$

where ρ is the density, c is the specific heat, T is the temperature, z is the vertical coordinate, and t refers to time. The subscript s denotes values in the snow.

In addition to the penetration of short-wave radiation, conduction of heat in the ice is influenced by small pockets of brine trapped in the ice during bottom accretion. The brine is assumed to be at its freezing point and in phase equilibrium with the surrounding ice. The equilibrium is maintained by volume changes in the brine pocket. A rise in temperature causes the ice surrounding the pocket to melt, which dilutes the brine and raises its freezing point to the new temperature. The brine pocket is thus a thermal reservoir that retards the heating or cooling of the ice. It is clear that the bulk thermal constants of the ice must be functions of both temperature and salinity.

The variations of density, conductivity, and specific heat were first investigated by *Malmgren* [1927], and a thorough theoretical analysis of the problem has been presented by *Schwerdtfeger* [1963]. *Untersteiner* [1961] introduced the following approximate formulas to describe these variations

$$(\rho c)_i = (\rho c)_{i,f} + \frac{\gamma S(z)}{(T - 273)^2} \qquad (3)$$

and

$$k_i = k_{i,f} + \frac{\beta S(z)}{T - 273} \qquad (4)$$

where $S(z)$ is the ice salinity at a depth z; $\gamma = 4100$ cal °K/g and $\beta = 0.28$ cal cm²/g sec are constants. The subscript f refers to pure ice and $(\rho c)_{i,f} = 0.45$ cal cm³ °K, and $k_{i,f} = 0.00486$ cal/cm sec °K. *Ono* [1967] derived theoretical expressions for $(\rho c)_i$ and k_i. The resulting equations, although slightly more complex than Untersteiner's, proved to be similar in form and to give values that are in remarkably good agreement. For simplicity, (3) and (4) were chosen for use in this model.

Untersteiner [1964] derived a complete description of energy transfer within the ice:

$$\left[(\rho c)_{i,f} + \frac{\gamma S(z)}{(T - 273)^2}\right] \frac{\partial T}{\partial t}$$

$$= \left[k_{i,f} + \frac{\beta S(z)}{T - 273}\right] \frac{\partial^2 T}{\partial z^2} + \frac{\beta}{T - 273} \frac{ds}{dz} \frac{\partial T}{\partial z}$$

$$- \frac{\beta S(z)}{(T - 273)^2} \left(\frac{\partial T}{\partial z}\right)^2 + I_0 \kappa_i \exp(-\kappa_i z)$$

$$- \left[(\rho c)_{i,f} + \frac{\gamma S(z)}{(T - 273)^2}\right] w \frac{\partial T}{\partial z} \qquad (5)$$

where w is the upward velocity of ice due to thickness changes at the boundaries, and the subscript i refers to variables in the ice. Solution of this equation, with specified boundary temperatures, provides a temperature field consistent with observations.

An examination of (5) reveals that several terms may be dropped without substantial loss of accuracy. The last term, a vertical advection term describing the heat transport associated with hydrostatic displacement of the ice, is small and was eliminated. Its removal allows the upper and lower boundaries to move independently of one another; i.e., there is no hydrostatic adjustment. An order-of-magnitude analysis indicates that the terms $\beta/(T - 273)\, dS/dz\, \partial T/\partial z$ and $[\beta S(z)/(T - 273)^2](\partial T/\partial z)^2$ are 3 orders of magnitude smaller than the major terms. Removal of these terms is equivalent to assuming that conductivity is constant within an incremental layer of thickness Δz. This assumption is consistent with a finite-difference solution and still allows the equation to consider variations in conductivity from layer to layer. With the above simplifications (5) becomes

$$\left[(\rho c)_{i,f} + \frac{\gamma S(z)}{(T - 273)^2}\right] \frac{\partial T}{\partial t}$$

$$= \left[k_{i,f} + \frac{\beta S(z)}{T - 273}\right] \frac{\partial^2 T}{\partial z^2} + \kappa_i I_0 \exp(-\kappa_i z) \qquad (6)$$

(6) is now the basic equation describing heat flow in the ice.

When snow covers the ice we assume at the ice/snow interface ($z = h$) that $T_s = T_i$ and that conduction is continuous through it, i.e.,

$$k_s \left(\frac{\partial T_s}{\partial z}\right)_h = k_i \left(\frac{\partial T_i}{\partial z}\right)_h \qquad (7)$$

At the bottom of the ice there are only two fluxes to be considered: the turbulent heat flux from the ocean and the conductive heat flux in the ice close to the boundary. The magnitude o

the two fluxes is similar, with one or the other dominating during different seasons. The boundary equation has the form

$$k_i\left(\frac{\partial T_i}{\partial z}\right)_{z=0} - (\rho c)_w K_w \left(\frac{\partial T_w}{\partial z}\right)_{z=0} = \left[\eta \frac{d}{dt}(h + H)\right]_{z=0} \qquad (8)$$

where K_w is the coefficient of eddy diffusivity in the water, the subscript w refers to values in the water, and h and H are the thicknesses of snow and ice. Without a theoretical model of the ocean, it is not possible to calculate the heat flux from the water. Thus $(\rho c)_w[K_w(\partial T_w/\partial z)]_{z=0}$ is specified as an external parameter, and bottom growth is determined by the model. For convenience, we adopt the following notation throughout the remainder of the text:

$$F_w = (\rho c)_w \left(K_w \frac{\partial T_w}{\partial z}\right)_{z=0}$$

Solution of (1), (2), (6), and (8) give temperatures in the snow and ice and mass changes at the upper and lower boundaries (Figure 1).

The equations were numerically evaluated on an IBM 7090/7094 system by using a stable alternating direction explicit method [*Saul'ev*, 1957*a*, *b*; *Larkin*, 1964]. For a given space increment this method allows a time increment roughly an order of magnitude greater than that allowed by the standard forward-difference method [*Richtmyer*, 1957]. The usual grid spacings used in the solutions discussed below were 10 cm and 12 hours. Winter temperatures at the upper boundary were calculated from (1) by the Newton-Raphson iterative procedure. For a complete discussion of the numerical techniques, see *Maykut and Untersteiner* [1969].

Input Parameters

Energy fluxes. As with any parabolic equation, initial conditions (temperature and thickness) and boundary values (energy fluxes) for each time increment must be specified. The energy fluxes are functions of time but repeat themselves in a constant annual cycle. Integration forward in time eventually yields steady-state annual patterns of temperature and thickness, i.e., the ice is in equilibrium with its environment. In the present instance, equilibrium is assumed to exist when the annual ice ablation at the upper surface approaches within ±0.1 cm of the annual net bottom accretion. In the initial integration of the model values that closely resemble actual conditions in the central Arctic were chosen; results could then be compared with observations as a test of the validity of the model.

At the upper boundary, four energy fluxes must be specified: F_s, F_l, F_e, and F_c. Values for these quantities have been suggested by *Vowinckel and Orvig* [1966, 1967] and by *Donn and Shaw* [1966]; however, their estimates pertain to the entire Arctic Ocean, including leads, ridges, melt ponds, and so forth and are therefore not applicable to a one-dimensional model. The heat balance proposed by *Fletcher* [1965] is based on the largest amount of observational data taken on perennial sea ice and was therefore chosen as the most appropriate. Following the suggestion of *Fletcher* [1965], the values given by *Marshunova* [1961] for F_l and F_e and those by *Doronin* [1963] for F_s and F_c were selected (Table 1). Values for each time increment were obtained by assuming that the monthly values were representative of the middle of each month and by then applying a polynomial smoothing function.

During the snow-free summer months, solar radiation penetrating the ice surface (I_0) is the principal source of internal heating. Temperature profiles taken at the height of the melt season indicate an internal heating of the slab of approximately 700 cal/cm² in only 14 days [*Untersteiner*, 1961]. The temperature gradient (and therefore the conductive heat fluxes) remained nearly constant during this period, implying that the observed heating resulted from I_0, rather than from conduction. Untersteiner's data indicate that about 32% of the net shortwave radiation makes no direct contribution to surface melting. On the basis of these observations, *Untersteiner* [1961] arrived at an annual value for I_0 of 1.2 kcal/cm². Imposing the restriction that I_0 total 1.2 kcal/cm² during the snow-free period on Fletcher's suggested heat budget means that only 17% of the net shortwave radiation may penetrate the ice. This is in apparent conflict with Untersteiner's 32%, and it is possible that his 1961 value underestimates I_0. In the initial trial of the model we tentatively accepted the latter value and assumed that 17% of the net short-wave radi

TABLE 1. Average Monthly Values for the Input Data at the Upper Boundary Compiled by *Fletcher* [1961]

Symbol	Variable	Jan.	Feb.	March	April	May	June	July	Aug.	Sept.	Oct.	Nov.	Dec.	Year
F_r	Incoming short-wave radiation, kcal/cm²	0	0	1.0	9.9	17.7	19.2	13.6	9.0	3.7	0.4	0	0	75.4
F_L	Incoming long-wave radiation, kcal/cm²	10.4	10.3	10.3	11.8	15.1	18.0	19.1	18.7	16.5	13.9	11.2	10.9	166.0
F_s	Flux of sensible heat, kcal/cm²	1.18	0.76	0.72	0.29	−0.45	−0.39	−0.34	−0.40	−0.17	0.10	0.66	0.79	2.71
F_l	Flux of latent heat, kcal/cm²	0	−0.02	−0.03	−0.09	−0.46	−0.70	−0.64	−0.06	−0.39	−0.19	−0.01	−0.01	−3.20
α	Surface albedo	...	...	0.83	0.81	0.82	0.78	0.64	0.69	0.84	0.85	...	...	...

tion passes through the surface and is absorbed within the interior of the ice. The extinction coefficient (κ_i) was assumed to be 0.015 cm^{-1} [*Untersteiner*, 1961; *Cherniqouskii*, 1966] and independent of depth.

Because of the difficulty in direct measurement, the magnitude of the oceanic heat flux (F_w) is not precisely known. Present estimates all depend on indirect evidence. The large values suggested by *Malmgren* [1927] and *Mosby* [1963] are considered unreliable because of some conceptual errors contained in their calculations. Independent calculations by *Crary* [1960], *Badgley* [1961], *Parow* [1964], and *Untersteiner* [1964] indicate that the average value must lie close to 1.5 kcal/cm² yr. Lacking more precise information, this value was chosen and assumed to remain constant throughout the year.

Albedo. The surface albedo (α) is probably the most important regional factor affecting the heat and mass budgets of the arctic pack ice. During the spring and fall, when surface conditions are uniform, α is high and relatively constant. A critical transition occurs during June and July, when there is a sharp increase in available energy and wide albedo fluctuations occur in response to the changing micro-relief of the surface. Most authors agree on spring and fall values for α, but disagree on summer averages. The problem arises because snow patches, bare ice, and melt ponds, all with different radiative characteristics, may coexist over a relatively small area. Occasional summer snowfalls can drastically alter the albedo for short periods. It is obviously impractical to attempt to duplicate such random fluctuations and horizontal variations in a one-dimensional model, so some realistic average must be used.

Untersteiner [1961] assumed an average albedo of 0.65, whereas Soviet measurements indicate a value of 0.64 [*Marshunova*, 1961; *Cherniqouskii*, 1966]. Unpublished data from Arlis-II show hourly albedo values fluctuating from 0.55 to 0.70 on melting ice. *Vowinckel and Orvig* [1966, 1967], on the other hand, hold a value of 0.45 to be representative. This view is supported by the fact that albedo measurements on melting, dirty ice have often been as low as 0.45, and integrated values from a 15-meter tower are even lower [*Langleben*, 1966]. These facts, combined with the prevalence of melt ponds, make Vowinckel's estimate appear

reasonable; however acceptance of a value this low is incompatible with other considerations. Energy balance calculations show that the net short-wave radiation resulting from an albedo of 0.43 would cause nearly 120 cm of ice ablation during the summer, an amount roughly three times the observed quantity.

Neglecting the influence of melt ponds, the average ice albedo is certainly closer to 0.64 than to 0.43. The albedo of the melt ponds is substantially lower than that of the ice, and the question that must be considered is how the increased ablation under the melt ponds affects the average ice thickness over an annual cycle. A melt pond at the end of the ablation season will freeze during the fall and, except for acting as a heat source to retard cooling, has little effect on annual thickness. During the summer, however, at least half of the melt ponds drain, forming channels and hollows in the surface topography. Snow accumulated in these depressions remains longer, retards ablation in these areas, and tends to level the ice relief. Increased ablation in melt ponds, therefore, has only a limited effect on the general ice thickness. In consequence, averages over large areas were set aside, and the albedo of the melting ice was taken as 0.64. The other albedos in Table 1 were also taken from *Marshunova* [1961].

Snow cover. Although surface irregularities such as pressure ridges cause some small-scale variations, snow depth is generally uniform throughout the central Arctic. To represent the present pattern of snowfall [*Untersteiner*, 1961; *Hanson*, 1965], we assumed a linear accumulation of 30 cm between August 20 and October 30, a linear increase of 5 cm from November 1 to April 30, and an additional 5 cm during the month of May. Where the summer melt season extends past August 20, snow accumulation is delayed until freeze-up occurs. If the surface temperature reaches the melting point before June 1, snow accumulation is cut off before it reaches 40 cm.

The fine-grained structure of arctic snow, combined with compaction by the wind, gives it a fairly high density. A value of 0.33 g/cm³ [*Untersteiner*, 1961] was chosen for the model. We assumed that the snow density (ρ_s) is independent of depth and remains constant as long as the snow temperature remains below freezing. At the onset of melting, the density increases rapidly to a limiting value of about 0.45 g/cm³ as melt water penetrates the snow and is refrozen. A precise treatment of the melting process would be difficult; however, a simple calculation reveals that, at the onset of snow melt, only an additional 50 cal/cm² are required to bring the entire layer up to the melting temperature. This is equivalent to the refreezing of only 2 cm of melted snow. The model preserves the essential features of the densification process by first allowing these 2 cm of snow to melt and then assuming that refreezing of the percolating meltwater and settling of the whole snow pack increases its temperature to the melting point and its density to 0.45 g/cm³.

Thermal conductivity (k_s) is quite variable, even in snows of equal density, and depends upon grain size, snow structure, and the temperature gradient. The formula of *Abels* [1892], $k_s = 0.0068\rho_s^2$ (cal/cm sec °K), represents a reasonable compromise of many diverse measurements and was used in the present model. Surface albedo during the transition from a snow cover to bare ice is assumed to be a function of snow depth, varying linearly between the value at the onset of melting and the bare ice value (0.64).

Salinity. Ice salinity becomes important in the calculation of the thermal constants at temperatures near the freezing point, where $(\rho c)_i$ may change by 2 orders of magnitude and k_i by 10%. Ideally, salinity should be described as a function of growth rate and thermal history of the slab; however, a proven theory of desalination is lacking [*Untersteiner*, 1968], and it is difficult to guess how the profile would change under varying conditions of temperature and speed of growth. Fortunately, an examination of (3) and (4) reveals that, unless the temperature is higher than −2 or −3°C, salinity has only a small effect upon $(\rho c)_i$ and k_i. Thus it is important only that salinity be known accurately during the summer and in the vicinity of the ice/water interface. Salinity in the lower portion of the ice is relatively constant at around 3.2 ppt. In the absence of more extensive data, the best documented equilibrium profile [*Schwarzacher*, 1959] was adopted to represent mean annual conditions. This profile is approximated by the expression

$$S(z, t) = A + B \sin\left[C\left(\frac{z}{H}\right)^{m/(z/H)+n} + D\right]$$

where H is the thickness of the ice, z is the depth, and A, B, C, D, m, and n are empirically determined constants. The equation, although complex, provides an extremely good fit to the data. Implicit in the equation is the assumption that the shape and end-points of the profile are retained during all fluctuations of ice thickness.

Other assumptions. For convenience, the year was divided into twelve months of 30 days each. Because both ice and snow radiate in the long-wave region much like a blackbody [*Kellogg et al., 1964*], the long-wave emissivity (ϵ_L) in (1) was set equal to unity. (3) and (4) show that both $(\rho c)_i$ and k_i are discontinuous at $T = 273°K$. To avoid this singularity, the melting temperature was assumed to be 273.9°K, which is realistic because a residue of salt remains in the upper layers of the ice. The temperature at the underside of the ice was assumed to remain constant at the freezing point of sea water (271.2°K).

LIMITATIONS

A basic shortcoming of the model is its inability to account for effects of mechanical stresses on the ice. Winds produce extensive deformation, as is evidenced by the occurrence of leads and pressure ridges [*Wittmann and Schule, 1966*] and are indirectly responsible for the export of large quantities of ice from the Arctic basin. If mechanical deformation adds a significant contribution to the amounts of ice stored in the Arctic, then predictions from the model can be used in mass budget studies only with suitable assumptions concerning the volume of ridged ice and the areal coverage of leads. It would be relatively simple to incorporate an export factor into the equations; however, no quantitative data exist on the distribution of ice sources.

Although mechanical motions influence the volume of ice contained in the Arctic, they affect ice growth only indirectly, and the factors of principal concern here are those which directly influence the energy budget. In equations 1 and 8, F_s, F_l, and F_w were assumed to be independent of growth rate and the physical state of the ice at the boundaries. This assumption is certainly not realistic for thin or rapidly growing ice and, ideally, these fluxes should reflect conditions at both surfaces. But unless theoretical models of the ocean and atmosphere can be incorporated into the boundary conditions, their effects must be specified as external parameters, and the outcome will be that the environment influences the ice, but not vice versa.

In addition to imprecise treatment of the downward heat transport from melting snow and the shape of the salinity profile, no provision has been included to account for the heat released by freezing of the melt ponds. The complete freezing of a 40-cm deep melt pond releases nearly 3 kcal/cm². An addition of heat of this magnitude could significantly increase upper level temperatures, decrease bottom accretion, and prolong the period of bottom ablation; the extent of these effects depends upon pond depth, areal coverage, and freezing time. Another limitation arises from the coarseness of the input data. Since the model requires energy fluxes at daily or hourly intervals, the monthly averages must be broken up into smaller increments by a smoothing process. Consequently the results will reflect the smoothing, and short-term trends or reversals will be absent. Finally, we stress that the model requires an existing layer of ice in order to function and hence cannot predict whether the ice will return once it has vanished.

INITIAL TEST OF THE MODEL

With the heat budget suggested by Fletcher (Table 1), with the other input data discussed in previous sections, and with an initial thickness of 340 cm, equilibrium was reached after 38 years. Figure 2 illustrates the steady-state temperature and thickness patterns for this condition. Since there is no hydrostatic term in (6), mass changes of each boundary are indicated separately (Table 2). The model predicts an average equilibrium thickness of 283 cm with a maximum of 314 cm and a minimum of 271 cm. It is difficult to assess how representative these values are. Early submarine data [*Lyon, 1961*] indicate an average thickness of 4 to 5 meters, but this includes pressure ridges and may be biased by the location of the sub

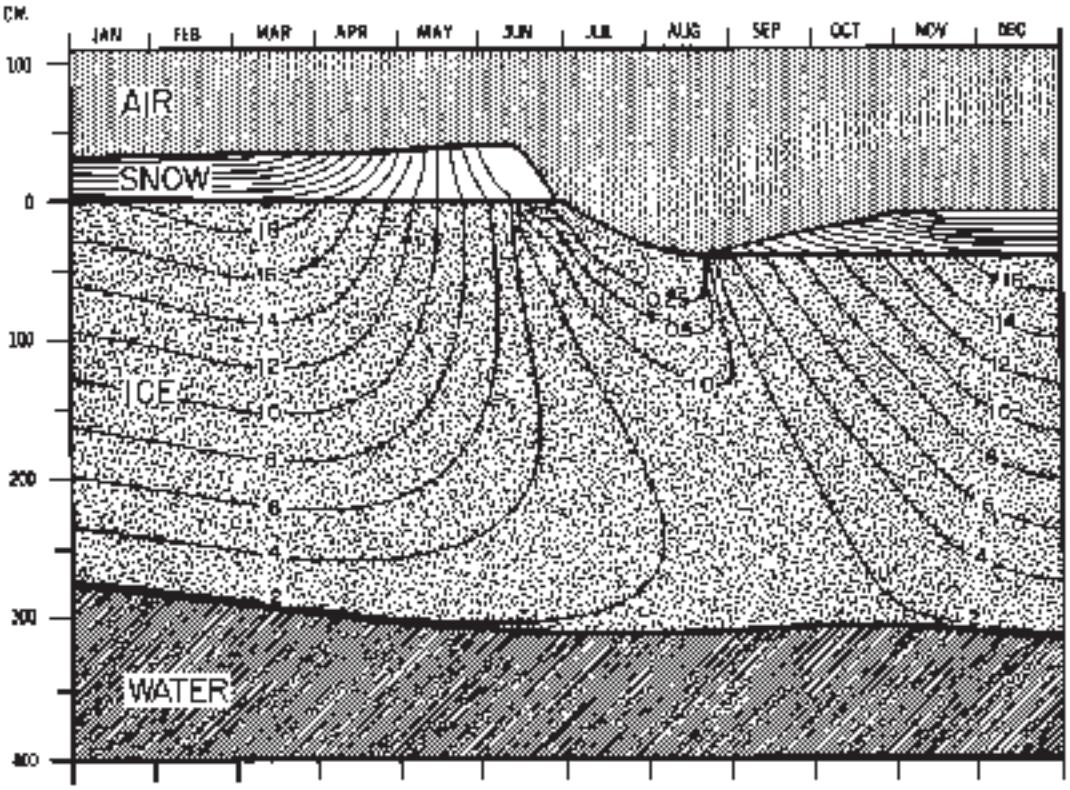

Fig. 2. Predicted values of equilibrium temperature and thickness for sea ice, based on Fletcher's heat budget for the central Arctic basin (Table 1). Isotherms in the ice are labeled in negative degrees Celsius; isotherms in the snow (unlabeled) are drawn at 2°C intervals. To distinguish between movements of the upper and lower boundaries, they are plotted without regard to hydrostatic adjustment. The vertical coordinate therefore corresponds to ice thickness only before the onset of ice ablation at the upper surface.

marine's track. Later submarine observations [*Wittmann and Schule*, 1966] show 2 meters to be the most frequent ice thickness, but again, these data are regionally limited. Most of the drifting stations were established on pack ice, which averaged close to 3 meters in thickness [*Petrov*, 1954]. Typical results are those of *Untersteiner* [1961] who found that thickness varied between 250 and 315 cm during the year. Considering that the input data are derived from those drifting stations, it is to be expected that the predicted thicknesses should agree most closely with their observations.

Perhaps more indicative is the pattern of mass changes predicted by the model. According to Soviet data [*Vowes*, 1966], average ablation on polar ice is 37 cm; snow melt begins in the first half of June and ablation generally ends between August 10 and 23. An average from all U.S. drifting stations from 1957 to 1963 gives a mean surface ablation of 42 cm [*Hanson*, 1965]. Table 2 shows a predicted ice ablation of 4 cm, starting on June 29 and terminating o August 19. Snow melt begins on June 8. At th lower surface there are 43 cm of accretion an 5 cm of ablation. Unfortunately, mass change at the bottom have never been well determine in the field. According to *Vowes* [1966] botto ablation in equilibrium ice is small, if it occu at all. *Hanson* [1965] measured a value of 1 cm, and *Untersteiner* [1961] observed 20 cm ablation and 50 cm of accretion. In view of thes uncertainties, the predicted values at the botto of the ice are not unreasonable, but a preci evaluation is not possible.

An observed temperature field [*Untersteine* 1961] is reproduced in Figure 3. Comparison Figures 2 and 3 shows good agreement through out, except for fall temperatures within the ic suggesting that ice temperatures in the theo retical model respond to surface conditions mo rapidly than do the temperatures in real ic

TABLE 2. Computed Values for Equilibrium Conditions in the 'Standard Case' (see Figure 2), Fletcher's Heat Budget (Table 1)

	Jan.	Feb.	March	April	May	June	July	Aug.	Sept.	Oct.	Nov.	Dec.	Year
Mean snow surface temperature, −°C	31.0	33.1	31.9	22.5	9.4	0.3	0.1	1.1	10.0	20.4	28.7	30.3	18.2
Mean ice surface temperature, −°C	18.0	19.0	19.2	15.8	9.7	2.8	0.1	0.9	6.2	10.7	14.8	17.2	11.2
Mean ice thickness, cm	282	289	297	304	310	314	306	278	273	271	271	276	288
Heat flux through surface, kcal/cm²	0.8	0.8	0.7	0.4	0	−0.1	0	0.2	0.7	0.8	0.9	0.8	6.0
Heat flux through bottom, kcal/cm²	−0.6	−0.6	−0.6	−0.6	−0.4	−0.3	−0.1	0	0	0	−0.3	−0.5	−4.0
Net short-wave radiation, kcal/cm²	0	0	0.4	1.9	3.1	4.4	5.0	2.7	0.6	0.1	0	0	18.2
Penetrating short-wave radiation, kcal/cm²	0	0	0	0	0	0.1	0.8	0.4	0	0	0	0	1.3
Net long-wave radiation, kcal/cm²	−2.0	−1.6	−1.8	−2.5	−2.2	−1.9	−0.9	−1.0	−0.7	−0.8	−1.4	−1.6	−18.4

Onset of			End of		Amount, cm		
Snow Ablation	Surface Ice Ablation	Bottom Accretion	Surface Ice Ablation	Bottom Accretion	Surface Ice Ablation	Bottom Ablation	Bottom Accretion
June 8	June 29	Nov. 4	Aug. 19	July 17	40.1	5.1	45.2

TABLE 3. Comparison of Observed and Calculated Surface Temperatures (−°C) for Sea Ice of Equilibrium Thickness

Source	Jan.	Feb.	March	April	May	June	July	Aug.	Sept.	Oct.	Nov.	Dec.	Year
Observed (screen height)	32.6	33.0	31.9	25.4	11.8	2.1	0.1	1.6	8.8	18.0	26.3	30.8	15.6
Calculated (surface)	31.0	33.1	31.9	22.5	9.4	0.3	0.1	1.1	10.0	20.4	28.7	30.2	16.2

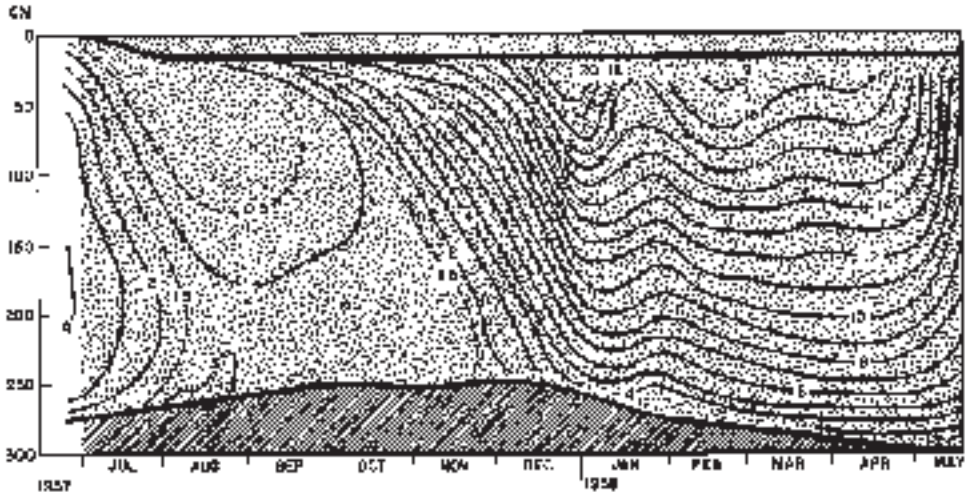

Fig. 3. Observed temperature and thickness pattern of perennial sea ice at IGY station alpha, 1957–1958 [after *Untersteiner*, 1961].

Neglecting latent heat release from surface melt ponds, underestimating I_0, or improper assumptions regarding the salinity profile could all contribute to this discrepancy. Smoothing of the input data is reflected in the results of Figure 2, and the usual January warming trend [*Lebedinow*, 1956; *Hisdal*, 1960] does not appear. Table 3 shows monthly surface temperatures from numerous drifting stations, averaged over 26 years of observations (A. Hanson, personal communication, 1957), and a comparison with the theoretical results. The annual averages are remarkably close, but temperatures predicted by the model are slightly colder in the fall and warmer in the spring than the observed ones. It should be remembered that the calculated temperatures apply for the surface, and a comparison with observed air (screen) temperatures would have to take into account that generally a ground inversion prevails from September to April, whereas in May lapse conditions prevail. We suspect, however, that the differences shown in Table 3 also result from the differing origins of the energy flux data and the observed temperature data.

Solar radiation absorbed by the surface in the model agrees closely with empirical data, implying that the albedo assumptions were adequate; however, the long-wave loss is somewhat smaller than observations indicate, primarily during the winter months [*Marshunova*, 1961]. This smaller loss appears to arise from two causes. First, the model deals only with thick ice covered with a uniform blanket of snow; observa tions in the field are made over ice with variab thickness and snow cover. Second, necessa smoothing of the input functions removes shor term fluctuations in the surface temperatur Because of the nonlinear form of the Stefa Boltzmann Law, this produces a bias towa lower surface temperatures and hence a small long-wave loss.

In a state of equilibrium, the sum of energy fluxes into the ice should balance t sum of those leaving it. The results in Table indicate that about 0.5 kcal/cm² yr more energ leaves the slab than enters it. This appare inconsistency is due to three energy sourc which are not seen explicitly in the outp data:

1. Short-wave radiation that penetrates t ice and is not absorbed, passing instead throug the ice and into the ocean. This flux is sma for thick ice (25 cal/cm² yr in the present case but for thin ice it may reach values in exce of 25% of I_0.

2. Latent heat released within the ice. As s water freezes at the bottom of the ice, smal pockets of brine are trapped. Continued accr tion moves the older ice upward into regions lower temperature, causing freezing in the brin pockets and a reduction in brine volume. Th resulting heat release is accounted for by chang in $(\rho c)_i$.

3. When the snow is saturated with wa

water and is isothermal, no heat flows toward the surface. The ice–snow interface, however, remains at the freezing point, causing a large conductive flux into the ice. The sudden introduction of this flux is responsible for the step seen in the −1.0, −0.5, and −0.25 isotherms during June (Figure 2).

Despite the many uncertainties in the input data, the picture presented by the model is surprisingly consistent with field observations. The model and the various approximations thus appear to be valid and lend confidence to the model's application to other possible situations.

Results of Selected Integrations

To investigate the effects of changes in such parameters as albedo, penetrating short-wave radiation (I_0), heat flux in the ocean (F_w), and snow depth on the growth of sea ice, numerous equilibrium solutions were obtained for different values of each parameter. Because results from the 'standard' case discussed earlier appear to be compatible with observations, the input data for this case have been adopted as the 'standard conditions.' One parameter is allowed to deviate from the standard conditions, and the model is then integrated until equilibrium is achieved. Some of the results are summarized below. The complete results are contained in a RAND Memorandum, RM-6093-PR [*Maykut and Untersteiner*, 1969].

Surface albedo. Because of the magnitude of the incoming solar radiation flux, a small reduction in surface albedo would provide a large increase in available energy at the surface. It has been speculated that the pack ice might be removed by artificially lowering its albedo through dispersal of some dark substance (like coal dust) on its surface. Although some small-scale albedo modification experiments have been conducted on sea ice [*Arnold*, 1961] to test the effectiveness of various dusting materials, it is not known how feasible such efforts would prove to be on a large scale.

To gain an appreciation of the sensitivity of ice thickness to albedo changes, we investigated two instances in which the albedo was lowered during the melt season (June–August) by 10% and 20%. The 20% lowering, corresponding to a bare ice albedo of 0.44, resulted in 120 cm of ice ablation during the summer and complete melting of the ice in the third summer. Wh the albedo was only lowered to 0.54, there w 78 cm of surface ice ablation, and the avera equilibrium ice thickness was 105 cm (Table and Figure 4). Comparison with the standa case shows an excess of net short-wave radi tion of 4 kcal/cm² yr, with an attendant thi ning of the ice of nearly 200 cm.

These results show that the large-scale albed reported by *Vowinckel and Orvig* [1966, 196 and by *Langleben* [1968] would cause the pa ice to vanish within a few years. If their valu are indeed representative of albedo averages the central Arctic, approximately 12 kcal/c yr of the absorbed short-wave energy does n participate directly in melting at the surfac and some explanation is needed to account f the ultimate disposition of this energy.

Penetration of short-wave radiation. *Unte steiner* [1964] has theoretically investigated t effect of I_0 on internal ice temperatures, b no previous work has related I_0 to equilibriu thickness. We assumed in the standard case th 17% (1.8 kcal/cm² yr) of the net short-wa radiation penetrates the ice during the snow free period. Four other solutions were obtain in which I_0 was specified to have values of 8.5, 25.5, and 34%; all other input data we unchanged from the standard case. The resul of two of these experiments are given in Fi ures 5 and 6 and Tables 5 and 6. Summaries the other cases are given in Table 7.

Contrary to what might be expected, equ librium thickness actually increases as mo radiation penetrates the ice (Figure 7). Becau the net short-wave radiation remains consta and a greater percentage of it is absorbed with the ice, less energy is available for melting the surface. The additional energy absorb within the ice causes slight additional warmi in the slab, but it is for the most part stored heat of fusion within the diluted brine. Becau there is little temperature change, the condu tive heat flux to the surface remains almo unchanged during the ablation season. Tables and 6 show that, as I_0 increases from 0 to 34 surface ablation decreases from 52.3 to 3 cm/yr. Less surface ablation means that the i must thicken to slow bottom accretion a maintain equilibrium.

As I_0 increases from 0 to 2.5 kcal/cm² yr, t annual surface temperature decreases by ab

TABLE 4. Computed Values for Equilibrium Conditions, Given a 10% Reduction in the Surface Albedo during June–August (see Figure 4)
(All other input data as in the 'standard' case.)

	Jan.	Feb.	March	April	May	June	July	Aug.	Sept.	Oct.	Nov.	Dec.	Year
Mean snow surface temperature, −°C	29.4	31.6	30.4	21.3	8.8	0.1	0.1	1.0	3.6	19.5	27.4	28.7	17.3
Mean ice surface temperature, −°C	10.9	12.4	12.5	10.9	5.0	0.3	0.1	0.7	5.1	7.1	9.0	10.1	6.9
Mean ice thickness, cm	107	120	132	142	149	142	96	64	60	89	81	94	105
Heat flux through surface, kcal/cm²	1.1	1.1	1.0	0.6	0.2	−0.1	−0.2	0.1	0.3	1.0	1.2	1.1	7.9
Heat flux through bottom, kcal/cm²	−0.9	−0.9	−0.9	−0.7	−0.4	0.1	0.3	0.4	−0.5	−0.8	−1.0	−1.0	−6.1
Net short-wave radiation, kcal/cm²	0	0	0.4	1.9	3.1	7.1	6.8	3.2	0.6	0.1	0	0	22.2
Penetrating short-wave radiation, kcal/cm²	0	0	0	0	0	0.7	1.0	0.5	0	0	0	0	2.2
Net long-wave radiation, kcal/cm²	−2.3	−1.9	−2.1	−2.7	−2.4	−2.0	−0.9	−1.4	−0.8	−1.0	−1.7	−1.0	−20.7

Onset of			End of			Annually, cm		
Snow Ablation June 1	Surface Ice Ablation June 12	Bottom Accretion Sept. 3	Surface Ice Ablation Aug. 21	Bottom Accretion June 12		Surface Ice Ablation 78.3	Bottom Ablation 15.1	Bottom Accretion 93.4

0.1°C, whereas the average temperature at th ice/snow interface decreases by 1°C. The maxi mum temperature change within the ice is 3°C Intuitively, it could be argued that an increase energy input of 2.5 kcal/cm² yr into the ic should cause average temperatures to rise, de spite an increase in thickness. An examination Tables 5 and 6 shows that, although the down ward heat input into the ice has increased by 2.5 kcal/cm² yr, the upward heat flux at th surface has increased by only 0.4 kcal/cm² yr This apparent contradiction is explained by th 28-cm decrease in bottom accretion that reduc the heat conducted into the ice by about 2 kcal/cm² yr. Thus the net energy input is onl 20% of the increase in I_0 and, except during th summer and fall, ice thickness determines th temperature profiles.

As was pointed out earlier, the model predic more rapid cooling in the fall than observation indicate. One possible reason for this is that w have underestimated I_0. Comparison of Figure 2, 3, and 6 shows that when I_0 is 34%, the te temperatures are in much better agreement wi empirical data than in the standard case: how ever, ice ablation at the surface is too small.

It is possible to increase surface ablatio while maintaining a large I_0 simply by decreas ing the albedo of the melting ice (α_i); α_i sufficiently in doubt that a small percenta change is acceptable. In the next case, α_i w reduced from 0.64 to 0.58, and I_0 specified 34%. Results are given in Table 8 and Figu 9. A comparison with the standard case show nearly the same surface ablation, but sol energy absorbed within the ice is greater by 1 kcal/cm² yr. Because mass changes at the su face have been separated from I_0, it now be comes possible to define how the ice respond to I_0 alone. Even though surface ablation re mains nearly constant, bottom ablation in th case is more than double that of the standa case. To maintain equilibrium, bottom accretio must therefore increase, but this may occur on if the ice thins. Average thickness is 229 cm that is, 60 cm less thickness for an annual energ increase of only 1.9 kcal/cm². Figure 9 show that an equivalent increase in F_w would cau the equilibrium thickness to decrease from 23 to 140 cm, thus illustrating the greater efficien of heat addition from the ocean.

The rate of cooling within the ice in autum

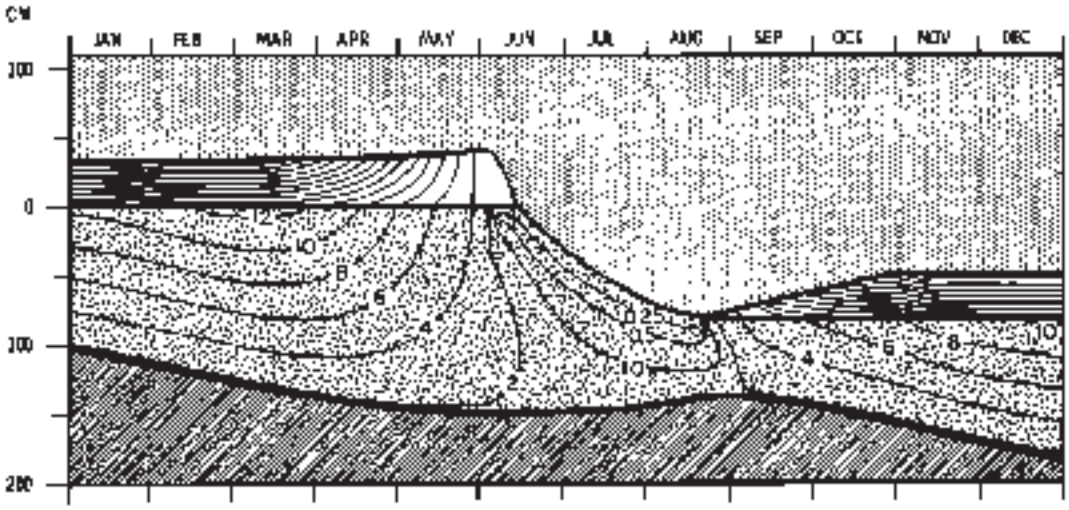

Fig. 4. Predicted values of equilibrium temperature and thickness for arctic sea ice, given a 10% reduction in the surface albedo during the summer ablation season (June–August). A 20% reduction resulted in complete disappearance of the ice during the third summer.

is considerably less than in the standard case. Surface temperatures are higher in the winter, but this is due to thinner ice. Fall temperature patterns in Figure 8 are similar to the observed ones (Figure 3); however, the cooling rate in the upper meter of the ice is still too high from September through December. It does not appear that a further increase in I_0 would be able to duplicate the pattern of Figure 3. Because the greatest discrepancy now occurs in the upper portion of the ice, the most likely explanation for the slower cooling in autumn is the later heat release from freezing melt ponds, possibly combined with an underestimation of I_0.

Although *Untersteiner* [1961] calculated a I_0 of 34% during the height of the melt season

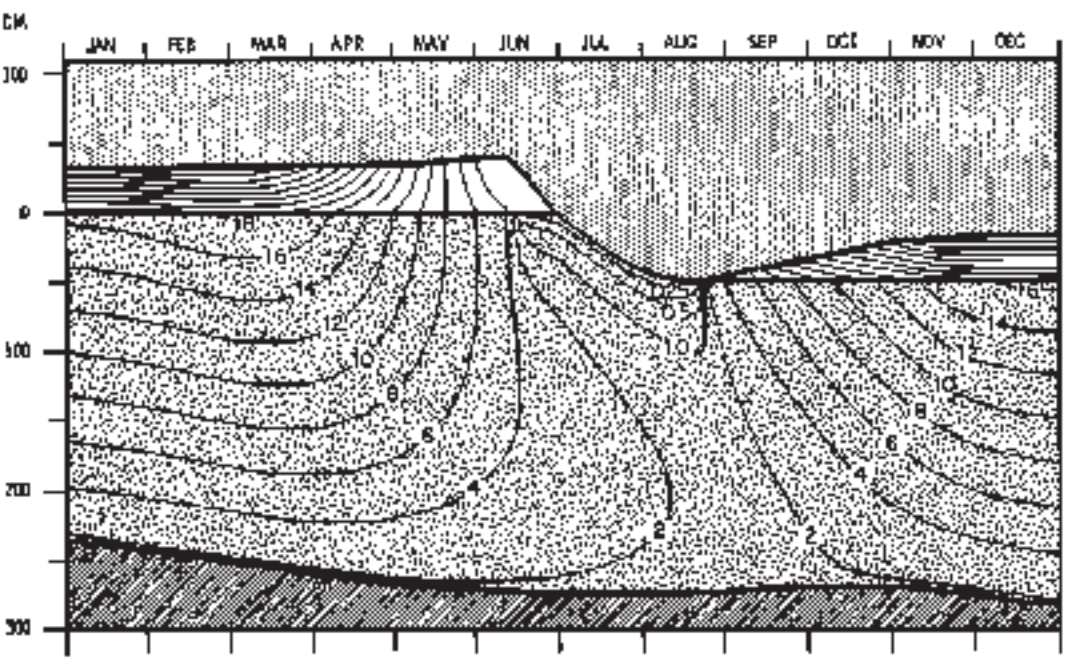

Fig. 5. Predicted values of equilibrium temperature and thickness for arctic sea ice when no solar radiation is allowed to penetrate below the surface of the ice. Fall cooling rates are much larger than those shown in Figures 3 and 8.

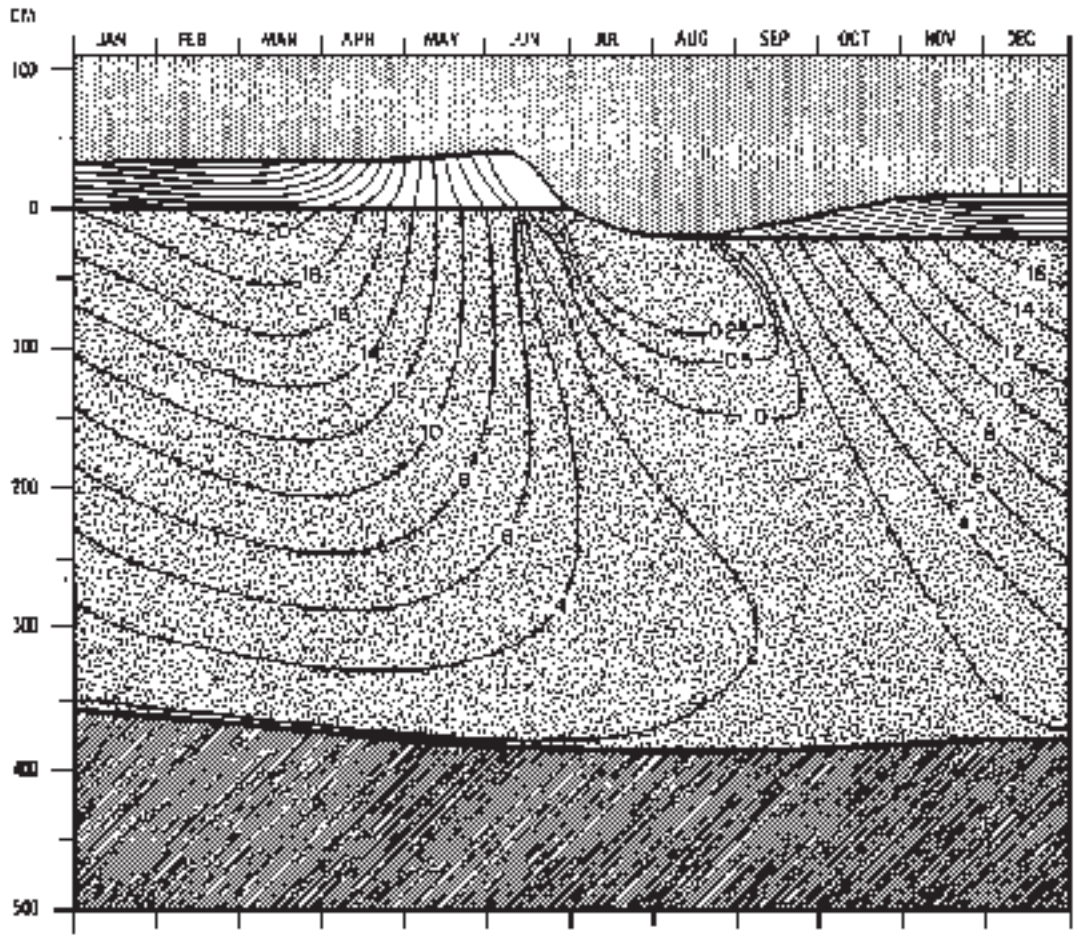

Fig. 6. Predicted values of equilibrium temperature and thickness for arctic sea ice when 30% of the net short-wave radiation is allowed to penetrate the ice during the snow-free period. Full cooling rates are similar to observations (Figure 5), however mass changes at the boundaries are smaller than observational averages.

and *Cherniqovskii* [1963] appears to have measured an I_0 of 47%, there are several objections to values this large. When I_0 is large, the combination of a 300 cm thickness and a surface ablation of 40 cm is impossible. If we accept less ice ablation, it is possible to have a reasonable ice thickness and a large I_0. Untersteiner, for example, measured only 32 cm of ice melt, which is consistent with his ice thickness and I_0 measurements.

These considerations demonstrate the need for careful studies of the relationship between I_0, net short-wave radiation, and surface ablation. Observations of the distribution and depth of melt ponds before and after the fall freeze-up would provide crucial information on their role in the temperature regime. Because it is still impossible to say which combination of I_0 and surface ablation is truly representative, the ar ceeding instances were again integrated with I_0 of 17%, conceding, however, that it may l larger.

Oceanic heat flux. Since the pioneering wo of *Malmgren* [1927], the turbulent transfer heat from the ocean to the ice has been subjec to numerous estimates and speculations. Wi variations in F_w are an integral part of sever theories of the ice ages, and numerous schem for artificially influencing the extent of the pa ice depend upon changing F_w [*Topornin*, 196 *Fletcher*, 1965]. The feasibility of any of the proposals is difficult to establish because of lack of quantitative knowledge regarding t sensitivity of ice response to F_w. It is not know how large the heat flux must become before t ice would vanish, and disagreement still exis

TABLE 5. Computed Values for Equilibrium Conditions When No Short-Wave Radiation Is Allowed To Penetrate the Surface during the Snow-Free Period ($I_0 = 0$)
(All other input data as in the 'standard' case.)

	Jan.	Feb.	March	April	May	June	July	Aug.	Sept.	Oct.	Nov.	Dec.	Year
Mean snow surface temperature, −°C	30.7	32.9	31.6	22.2	9.3	0.3	0.1	1.1	10.2	20.4	28.7	30.1	18.1
Mean ice surface temperature, −°C	16.8	17.8	17.9	14.6	8.7	2.0	0.1	1.0	6.7	10.9	14.6	16.3	10.6
Mean ice thickness, cm	238	247	255	259	270	272	260	225	220	219	223	230	243
Heat flux through surface, kcal/cm²	0.8	0.9	0.8	0.4	0	−0.1	−0.3	0	0.6	0.8	0.9	0.8	5.6
Heat flux through bottom, kcal/cm²	−0.7	−0.7	−0.7	−0.6	−0.4	−0.3	−0.1	0	0	−0.2	−0.5	−0.6	−4.8
Net short-wave radiation, kcal/cm²	0	0	0.4	1.9	3.1	4.4	5.0	2.8	0.6	0.1	0	0	18.3
Penetrating short-wave radiation, kcal/cm²	0	0	0	0	0	0	0	0	0	0	0	0	0
Net long-wave radiation, kcal/cm²	−2.0	−1.6	−1.9	−2.3	−2.2	−1.9	−0.9	−1.0	−0.7	−0.9	−1.4	−1.6	−18.5

Onset of			End of		Amount, cm		
Snow Ablation	Surface Ice Ablation	Bottom Accretion	Surface Ice Ablation	Bottom Accretion	Surface Ice Ablation	Bottom Ablation	Bottom Accretion
June 7	June 28	Oct. 7	Aug. 22	July 13	52.3	3.4	55.7

TABLE 6. Computed Values for Equilibrium Conditions when 31% of the Net Short-Wave Radiation Is Allowed to Penetrate the Ice during the Snow-Free Period (see Figure 6)
(All other input data as in the 'standard' case.)

	Jan.	Feb.	March	April	May	June	July	Aug.	Sept.	Oct.	Nov.	Dec.	Year
Mean snow surface temperature, −°C	31.2	33.4	32.2	22.8	9.7	0.4	0.1	0.9	9.3	20.2	28.7	30.3	18.3
Mean ice surface temperature, −°C	18.7	20.0	20.8	17.5	11.2	2.9	0.1	0.5	4.5	10.0	14.5	17.3	11.5
Mean ice thickness, cm	360	364	370	376	382	385	370	364	362	361	359	358	368
Heat flux through surface, kcal/cm²	0.7	0.8	0.6	0.3	−0.1	−0.1	0.1	0.4	0.9	0.8	0.9	0.8	6.1
Heat flux through bottom, kcal/cm²	−0.4	−0.5	−0.5	−0.5	−0.4	−0.3	−0.2	−0.1	0	0	0	−0.1	−3.0
Net short-wave radiation, kcal/cm²	0	0	0.4	1.9	3.1	4.4	5.0	2.7	0.6	0.1	0	0	18.2
Penetrating short-wave radiation, kcal/cm²	0	0	0	0	0	0.1	1.7	0.8	0	0	0	0	2.6
Net long-wave radiation, kcal/cm²	−1.9	−1.5	−1.7	−2.4	−2.1	−1.9	−0.9	−1.0	−0.9	−0.8	−1.5	−1.6	−18.2

Onset of			End of		Amount, cm		
Snow Ablation	Surface Ice Ablation	Bottom Accretion	Surface Ice Ablation	Bottom Accretion	Surface Ice Ablation	Bottom Ablation	Bottom Accretion
June 8	June 29	Dec. 14	Aug. 14	Aug. 1	24.7	6.0	30.7

TABLE 7. Summary of Annual Equilibrium Results for Various Values of Oceanic Heat Flux, F_w (kcal/cm² year), Maximum Snow Depth, h_m (cm), and Percentage of Net Short-Wave Radiation Penetrating the Ice during the Snow-Free Period, I_0

	'Standard' Case	$F_w = 0$	$F_w = 0.15$	$F_w = 5.0$	$F_w = 4.5$	$h_m = 0$	$h_m = 20$	$h_m = 60$	$h_m = 80$	$h_m = 100$	$h_m = 120$	$I_0 = 8.5\%$	$I_0 = 25.5\%$
Mean snow surface temperature, —°C	16.3	16.7	16.5	17.7	17.2	—	17.0	16.0	16.9	19.2	19.5	16.2	16.3
Mean ice surface temperature, —°C	11.2	13.5	12.4	9.7	0.0	10.5	12.1	9.6	9.9	9.9	9.3	10.9	11.4
Mean ice thickness, cm	238	661	391	159	93	800	310	288	317	411	703	202	234
Heat flux through surface, kcal/cm² yr	5.0	4.5	5.2	7.2	8.2	10.2	6.6	5.0	4.2	3.4	2.6	6.3	5.9
Heat flux through bottom, kcal/cm² yr	—4.2	—2.5	—3.5	—5.6	—6.9	—5.9	—4.7	—3.4	—2.8	—2.2	—1.5	—4.5	—3.6
Net short-wave radiation, kcal/cm² yr	18.2	18.0	18.1	18.3	18.8	22.7	18.6	17.8	17.8	16.8	16.3	18.2	18.1
I_0, kcal/cm² yr	1.3	1.2	1.3	1.3	1.8	3.0	1.0	1.0	0.8	0.6	0.1	0.7	1.0
Net long-wave radiation, kcal/cm² yr	—16.3	—17.1	—17.7	—19.7	—21.0	—22.9	—19.2	—17.6	—16.6	—15.9	—15.1	—16.4	—16.3
Onset of snow ablation	June 6	June 9	June 8	June 7	June 6	---	June 9	June 7	June 7	June 7	June 7	June 7	June 8
Onset of ice ablation	June 29	July 1	June 29	June 28	June 27	June 6	June 21	July 8	July 15	July 26	Aug. 13	June 28	June 29
End of ice ablation	Aug. 19	Aug. 19	Aug. 19	Aug. 18	Aug. 17	Aug. 19	Aug. 30	Aug. 10	Aug. 10	Aug. 19	Aug. 18	Aug. 21	Aug. 17
Onset of bottom accretion	Nov. 4	---	Nov. 10	Oct. 3	Sept. 7	Oct. 28	Nov. 2	Nov. 9	Nov. 24	Dec. 26	April 5	Oct. 19	Nov. 21
End of bottom accretion	July 17	---	Sept. 18	July 7	May 16	July 3	July 23	July 17	July 24	Aug. 14	Oct. 4	July 14	July 22
Surface ice ablation, cm	40.1	38.7	39.9	40.1	37.6	68.5	30.1	30.2	30.2	10.6	0.5	36.5	32.5
Bottom ablation, cm	5.1	0	0.5	16.7	26.5	6.4	4.3	5.6	4.5	3.4	2.1	4.5	5.6
Bottom accretion, cm	45.2	38.7	40.4	56.7	63.3	74.9	54.4	35.7	23.0	14.0	2.6	51.0	38.6

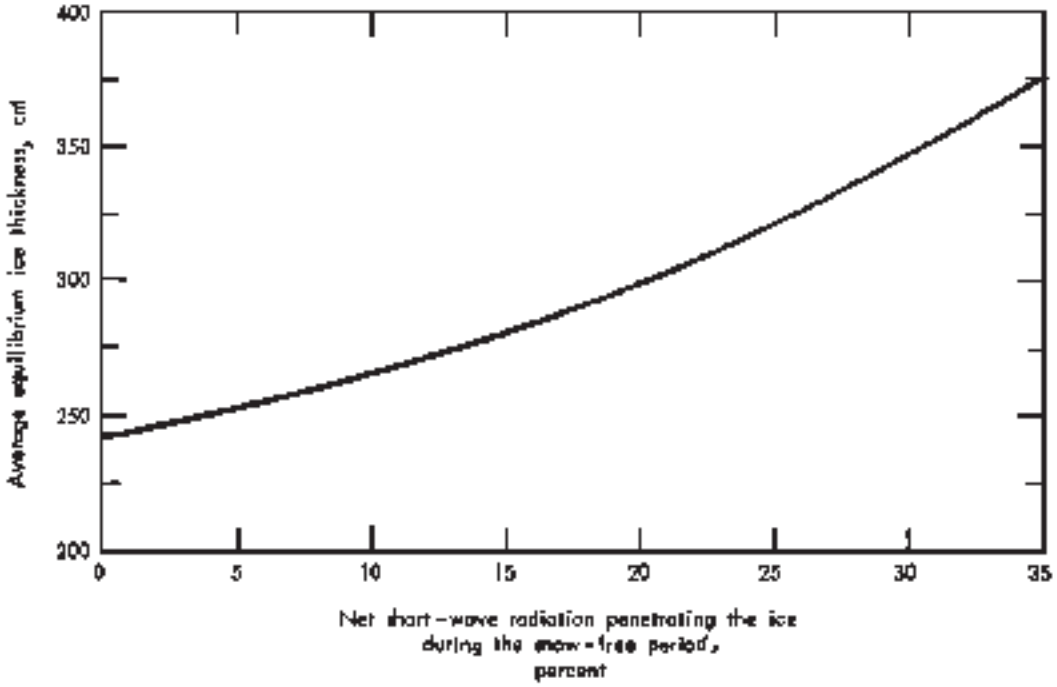

Fig. 7. Average equilibrium thickness of arctic sea ice as a function of the percentage of net short-wave radiation that penetrates the ice during the snow-free period.

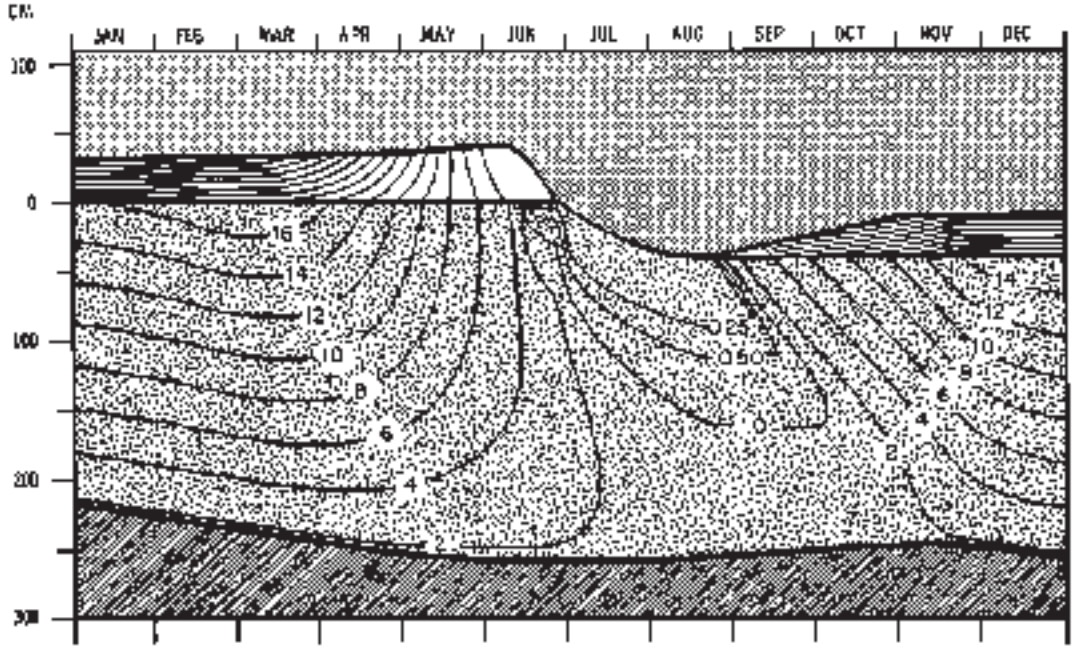

Fig. 8. Predicted values of equilibrium temperature and thickness for arctic sea ice when the summer ice albedo is assumed to be 0.53, and 34% of the net short-wave radiation is allowed to penetrate the ice during the snow-free period. Theoretical cooling rates and mass changes agree well with observations.

as to the present magnitude of F_w. In this section we will first describe the total response of the ice to changes in F_w, then determine an upper limit for F_w, and finally define a range of conditions under which the ice could currently exist.

Five examples were integrated by using annual values for F_w of 0, 0.75, 3.0, 4.6, and 6.0 kcal/cm² yr. Because no obvious inconsistencies had resulted from assuming that F_w remained constant throughout the year in the standard case, the other cases were computed under the same assumption. All other fluxes were left unchanged. A summary of annual equilibrium results is given in Table 7. When F_w was set equal to 6.0 kcal/cm² yr, the ice vanished before equilibrium could be established.

Figure 9 shows a graph of equilibrium thickness versus F_w; curves for seasonal maximum and minimum thickness and average thickness are drawn. When the ice is thicker, the average value is closer to the minimum, reflecting the decrease in bottom ablation. Under present surface conditions, the theoretical thermodynamic limit of ice thickness is about 660 cm, whereas the ice should vanish if F_w increases to 5 or 6 kcal/cm² yr.

Variations in oceanic heat flux have relatively little direct influence on processes occurring at the upper boundary. The surface temperature of ice 90 cm thick is up to 12°C higher than the surface temperature of 580-cm ice, but because the snow is an effective thermal insulator, average snow surface temperatures are only 2° or 3° higher. Similarly, because of the snow cover, the onset of snow and ice ablation changes by only 3 days. The amount of ice ablation at the upper surface varies by only a few centimeters because the quantity of heat conducted to the surface during the snow-free period is similar in all instances, indicating that temperature gradients during the summer are generally determined by the penetrating short-wave radiation, rather than by ice thickness. Bottom accretion unexpectedly begins earlier in the fall when F_w is larger. The predicted temperature fields indicate that in thin ice the lower portion responds more rapidly to temperature changes at the surface. Thus the steeper temperature gradients within the ice outweigh the effects of a higher F_w and result in earlier bottom accretion.

Most field observations indicate an average ice thickness between 250 and 350 cm, which corresponds in Figure 9 to values of F_w betwee 1.0 and 2.0 kcal/cm² yr. These values refer to 'effective' F_w. It is probable that more heat carried into the basin but is lost through lea [*Coachman*, 1966]. Because uncertainties th could also affect thickness exist in the oth input data, it is not possible to assign a speci value to F_w. However, on the basis of the te perature results, it is unlikely that errors in t energy fluxes at the upper surface could modi the thickness results by more than ±0.5m. Th being true, the estimates of oceanic heat fl by Crary, Badgley, and Untersteiner must very close to reality and the earlier ones consi erably in error.

Snow cover. A snow cover insulates the i from the cold air and reflects much of the i coming short-wave radiation. The effects snow on surface ablation and ice temperatur suggests that small changes in snow thickne might result in significant changes in equili rium thickness. The experiments described this section indicate that this is not true.

It was assumed in the standard case that t maximum snow depth under present conditio is 40 cm. To investigate the effects of variat snow thickness, 6 examples were integrat specifying maximum snow depths of 0, 20, 6 80, 100, and 120 cm. Snow was added in incr ments as previously described except that ea accumulation increment was multiplied by constant factor (0.5, 1.5, etc.) to bring t final snow depth up to the desired total. Exce for the no-snow instance, all other assum tions were consistent with the standard ca When snow was absent during the entire yea we assumed that $\alpha_s = 0.75$ if the surface tem perature was below freezing and 0.64 duri periods of surface melting. Figures 10 and and Table 9 present results from two of the experiments. Table 7 summarizes results fro the others.

Figure 12 shows the average equilibriu thickness as a function of maximum annu snow depth. For snow depths between 0 a 70 cm, the average ice thickness remains almo unchanged; above 70 cm, the thickness increas rapidly. To explain the unexpected shape this curve, it is necessary to examine the thr major variables that are influenced by t amount of snow: ice temperature, surfa ice ablation, and I_0. A thinner snow cov allows greater cooling of the ice during t

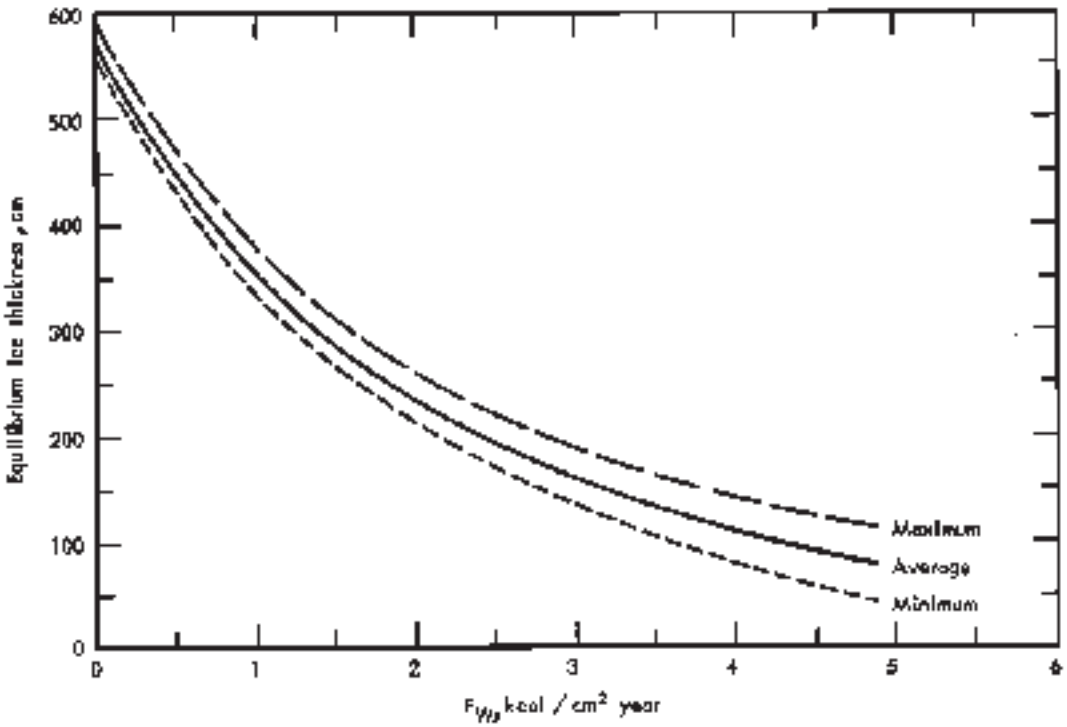

Fig. 9. Equilibrium thickness of arctic sea ice as a function of the annual value of the oceanic heat flux (F_w). Average annual ice thickness, as well as the absolute annual maximum and minimum, are shown. With the assumed energy budget, the ice vanishes during the summer when F_w is increased to 6 kcal/cm² yr.

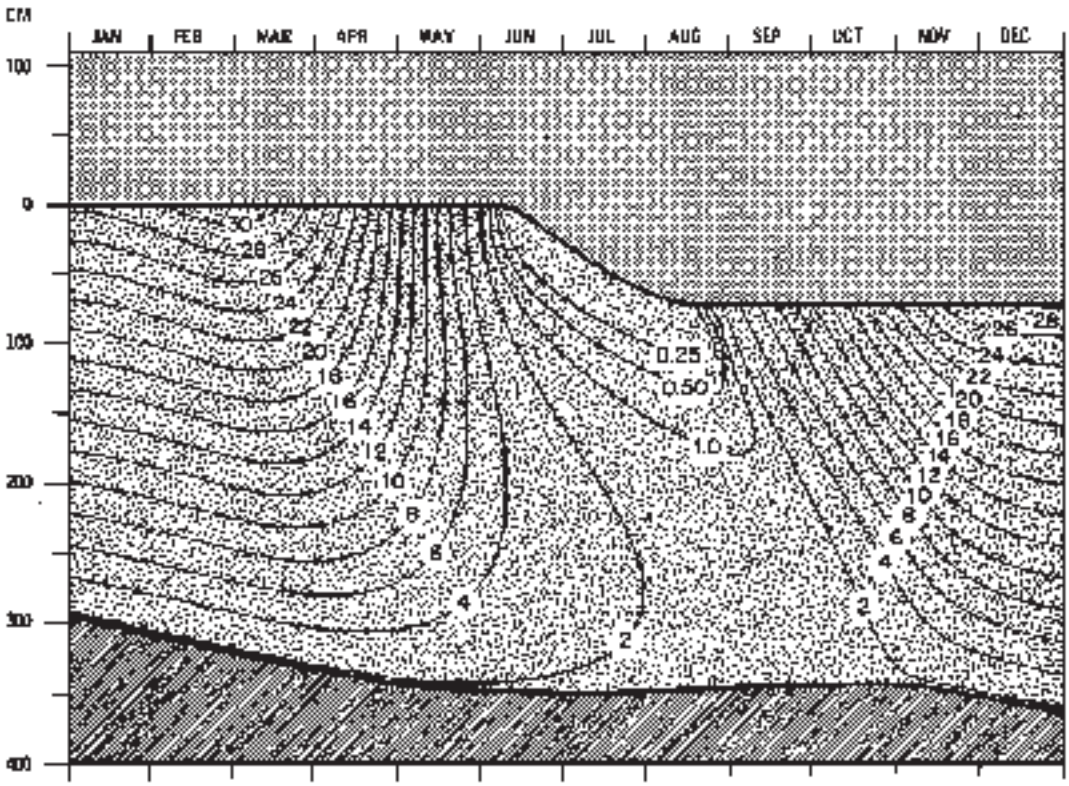

Fig. 10. Predicted values of equilibrium temperature and thickness for arctic sea ice in the absence of an annual snow cover. The albedo is assumed to be 0.75 when the surface temperature is less than −0.1°C and 0.64 when the ice is melting.

TABLE 8. Computed Values for Equilibrium Conditions When 34% of the Net Short-Wave Radiation Is Allowed To Penetrate the Ice during the Snow-Free Period and the Ice Albedo Is Assumed To Be 0.58 (see Figure 8)
(All other input data as in the 'standard' case.)

	Jan.	Feb.	March	April	May	June	July	Aug.	Sept.	Oct.	Nov.	Dec.	Year
Mean snow surface temperature, −°C	30.3	32.5	31.2	24.9	9.1	0.3	0.1	0.9	9.2	19.7	28.2	29.7	17.8
Mean ice surface temperature, −°C	15.1	15.1	15.2	13.1	7.6	1.6	0.1	0.5	4.2	8.3	12.7	14.6	9.2
Mean ice thickness, cm	192	200	209	217	223	225	204	186	178	175	175	183	197
Heat flux through surface, kcal/cm²	0.9	1.0	0.8	0.5	0.1	−0.1	0	0.4	0.9	0.9	1.0	0.9	7.3
Heat flux through bottom, kcal/cm²	−0.7	−0.8	−0.8	−0.6	−0.4	−0.2	0	0.2	0.1	0.1	−0.6	−0.7	−4.3
Net short-wave radiation, kcal/cm²	0	0	0.4	1.9	3.1	4.8	5.8	3.7	0.6	0.1	0	0	19.8
Penetrating short-wave radiation, kcal/cm²	0	0	0	0	0	0.3	2.0	0.9	0	0	0	0	3.2
Net long-wave radiation, kcal/cm²	−2.1	−1.7	−1.9	−2.6	−2.3	−2.0	−0.9	−1.0	−0.9	−0.9	−1.5	−1.7	−19.5

Onset of			End of		Amount, cm		
Snow Ablation	Surface Ice Ablation	Bottom Accretion	Surface Ice Ablation	Bottom Accretion	Surface Ice Ablation	Bottom Ablation	Bottom Accretion
June 7	June 28	Nov. 1	Aug. 18	June 29	39.7	12.6	52.3

TABLE 9. Computed Values for Equilibrium Conditions in the No-Snow Case; Ice Albedo Is Set Equal to 0.75 When the Surface Temperature Is Less than 272.2 °K (see Figure 10)
(All other input data as in the 'standard' case.)

	Jan.	Feb.	March	April	May	June	July	Aug.	Sept.	Oct.	Nov.	Dec.	Year
Mean ice surface temperature, −°C	28.5	30.4	29.4	20.7	7.3	0.2	0.1	0.7	7.8	17.4	25.7	27.8	16.3
Mean ice thickness, cm	274	288	298	310	317	308	273	252	248	255	260	261	277
Heat flux through surface, kcal/cm²	1.3	1.4	1.2	0.7	0.3	0	0	0.3	1.2	1.5	1.5	1.3	10.7
Heat flux through bottom, kcal/cm²	−1.0	−1.0	−1.0	−0.8	−0.5	−0.1	0	0	0.1	−0.1	−0.8	−1.0	−6.2
Net short-wave radiation, kcal/cm²	0	0	0.6	2.5	4.3	6.3	5.0	2.9	0.9	0.1	0	0	22.6
Penetrating short-wave radiation, kcal/cm²	0	0	0.1	0.4	0.7	1.1	0.9	0.5	0.2	0	0	0	3.9
Net long-wave radiation, kcal/cm²	−2.5	−2.1	−2.3	−2.9	−2.8	−2.0	−0.9	−1.1	−1.3	−1.5	−2.1	−2.1	−23.6

Onset of			End of		Amount, cm		
Snow Ablation	Surface Ice Ablation	Bottom Accretion	Surface Ice Ablation	Bottom Accretion	Surface Ice Ablation	Bottom Ablation	Bottom Accretion
—	June 5	Oct. 23	Aug. 19	June 28	68.2	6.6	74.8

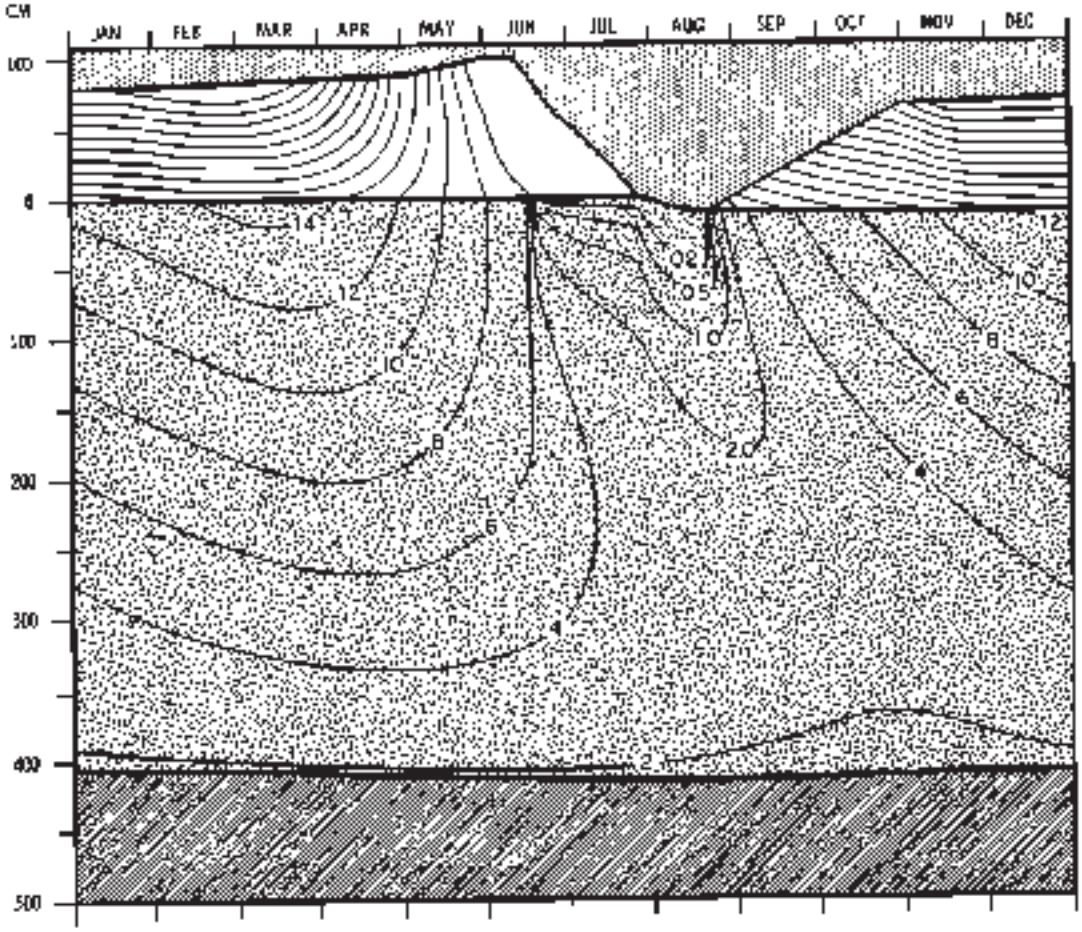

Fig. 11. Predicted values of equilibrium temperature and thickness for arctic sea ice, given an annual snow accumulation of 100 cm.

winter, promoting bottom accretion. If ice ablation at the surface remained constant, greater bottom accretion would lead to thicker equilibrium ice. However, when the maximum snow depth is less, the snow cover is removed earlier, thereby decreasing the average albedo and prolonging the period of ice ablation. Also, less energy is required to remove the thinner snow cover. With these effects ice ablation is greater, and more short-wave radiation is absorbed within the ice. Greater ice ablation at the surface tends to thin the ice but I_0 interacts with the ice in a more complex manner. Greater I_0 causes more bottom ablation, tending to thin the ice and to simultaneously deprive the surface of energy that could otherwise be used for melting. Thus there are four opposing effects: two that promote thickening and two that promote thinning. Figure 12 results from the balance of these effects. When maximum snow depth lies between 0 and 70 cm, there is mutual compensation between the thickening effects and the thinning effects; when the annual snow depth exceeds 70 cm, decreasing ice ablation and a smaller I_0 dominate the balance, and the ice thickens to maintain the balance.

These points are illustrated by the contr between the standard case and the no-sn instance, ice surface temperatures in the n snow instance are consistently lower, the ma mum difference being about 10°C, whereas t annual average differs by 5°C. Temperatu gradients within the ice are very steep duri the winter months (Figure 10), resulting in on more bottom accretion than the stands case. Because there is no snow to melt a because α_s is smaller than α_i, surface ice ab tion is greater by 28 cm. Although net sho wave radiation is 4.5 kcal/cm² yr higher, kcal/cm² yr of this excess is absorbed wit

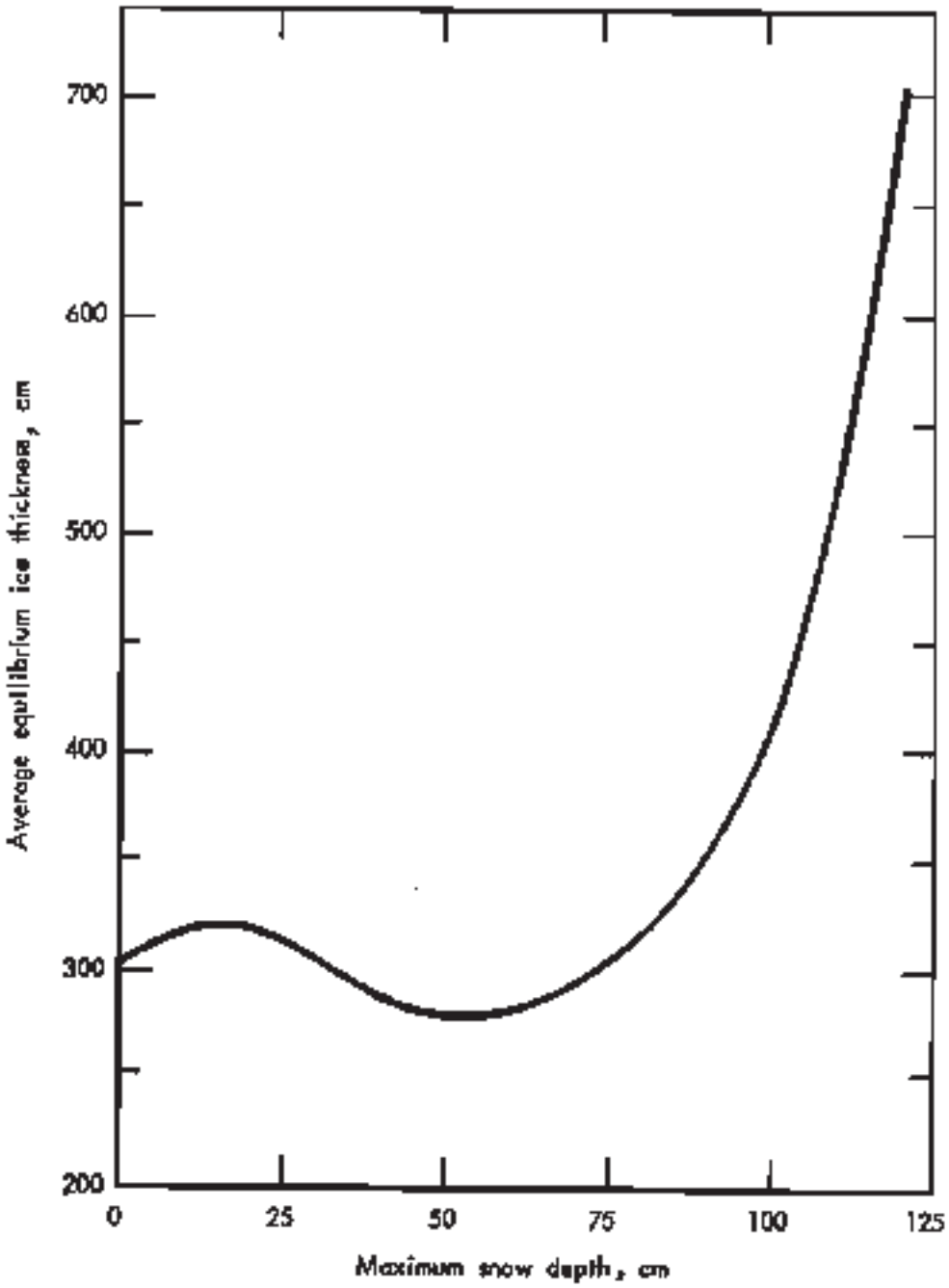

Fig. 12. Average equilibrium thickness of arctic sea ice as a function of maximum annual snow depth. Only with a drastic increase in snow cover do the insulating effects of the snow become large enough to produce a significant increase in ice thickness. Annual snow accumulations in excess of 120 cm result in incomplete melting of the snow cover and equilibrium sea ice would grow from above and ablate from below.

the ice, producing slightly more bottom ablation. Ice thickness during the spring is somewhat greater than in the standard case, but in the fall and early winter it is appreciably less. Thus, despite large differences in the mass changes at the boundaries, the annual energy balance and thickness of the slab are only slightly affected. A similar analysis of the other examples shows how less net short-wave radiation and the greater snow cover combine

reduce surface-ice ablation and I_0. The smaller energy input to the slab rapidly becomes the dominant influence and results in the predicted thickening of the ice.

Under the assumed energy input, the maximum snow depth that can occur without producing an annual surplus is 120 cm. If snow accumulation exceeds this amount, equilibrium ice will grow from above and ablate from below. The metamorphism of snow into ice cannot be handled by the present model. From this series of experiments, it appears that present variations in annual snowfall over the central Arctic have little effect on average ice thickness.

DISCUSSION

Infrared data [*Wittmann and Schule*, 1966] suggest that open water is so extensive in the Arctic that most of the heat transfer between the ocean and atmosphere would occur in these areas. Results from the model indicate that 1 to 2 kcal/cm² yr must be supplied to the ice by the ocean. It is estimated from sparse oceanographic data that only 2.0 to 2.5 kcal/cm² yr are advected into the central Arctic Ocean [*Crary*, 1960]. If the model is correct, it is not possible to reconcile Wittmann and Schule's observations and the oceanographic information with the present ice thickness. It seems probable that infrared techniques overestimate the amount of open water because they are not able to distinguish very thin ice from leads; however, further study is needed to clarify the problem.

Information about the penetration of short-wave radiation into the ice is generally deficient. This is unfortunate because the model has shown the extent to which I_s can influence ice temperature, ice thickness, and the annual pattern of mass changes at the boundaries. For a given oceanic heat flux, the equilibrium thickness is largely determined by the amount of surface ice ablation, which in turn is strongly influenced by the values of I_s and the albedo. To understand the interaction of solar energy with the ice, it is not sufficient to simply measure incoming and net short-wave radiation. The measurements should be combined with observations of surface ablation and calculations of I_0, preferably by both direct and indirect methods. Given the uncertainties in the current estimates of average ice thickness and ablation at the surface, it has not been possible to establish definitely the magnitude of I_0 from the model. On the basis of observed and calculated temperature profiles and the calculations of *Untersteiner* [1961], we are inclined to accept a value for I_0 of 2.0 to 2.5 kcal/cm² yr and a slightly lower summer ice albedo than suggested by *Maykut* (Table 1).

Representative surface albedos for the ice during the summer ablation season pose a major problem in treating the arctic energy budget. Although the model has shown that an albedo of 0.45 results in a rapid disappearance of the ice, there is some evidence that large-area averages for July may indeed be this low. This conflict must be explained by the way in which melt ponds and leads absorb energy and interact with the surrounding ice. Typical albedos range from 0.55 to 0.70 over melting ice, and from 0.20 to 0.35 over melt ponds; an integrated average must, of course, be lower than the value (0.64) assumed in the model. What needs to be clarified is the way in which melt ponds dispose of absorbed short-wave energy. A melt pond with an albedo of 0.20 absorbs about 3 kcal/cm² during July and August, 3 kcal/cm² more than the bare ice. Since melt ponds are usually about 40 cm in depth [*Untersteiner*, 1961], they have to lose roughly 5 kcal/cm² more energy during this period than the bare ice. This surplus energy may be lost through larger turbulent fluxes, more outgoing long-wave radiation, and, perhaps most important, greater I_0, but the magnitudes of the required increases are unknown.

Neither the energy budget of *Fletcher and Crary* [1966, 1967] nor that of *Fletcher* [1965] seems entirely satisfactory. The use of Fletcher's heat budget in the standard case produced remarkable agreement with observations. Paradoxically, it is for this reason that it cannot be considered truly representative of a large-scale average. By assuming an average summer surface albedo of 0.64, Fletcher neglects the effect of leads and melt ponds and underestimates the amount of short-wave radiation absorbed at the surface in the central Arctic. Although the extent of leads is uncertain, melt ponds cover 20 to 40% of the ice during July. Thus, 1 to 2 kcal/cm² yr more energy is absorbed at the surface than Fletcher assumes. However, year-to-year variations appear to be considerable

larger. The heat budget of Vowinckel and Orvig, on the other hand, appears to describe the gross features, but its quantitative accuracy remains to be verified because some of the energy fluxes are implicit in their formulation of the energy balance. For this reason their budget cannot be used to describe physical changes at the surface.

The most serious limitation in the present model lies in the simplifications made in stating the boundary conditions. The turbulent fluxes are dependent in part on conditions at the surface and should be parameterized in terms of gradients of humidity, temperature, and wind speed in the atmospheric boundary layer. In this way it might be possible to link this model to an atmospheric model. Before this is attempted, it may be more expedient as a next step to develop a suitable one-dimensional model of the oceanic convection under the ice and under a free water surface. Combined with the sea-ice model, this model would enable us to approach the central problem of the transition from an ice-free to an ice-covered state of the Arctic Ocean.

Acknowledgments. Thanks are due the RAND Corporation, Santa Monica, for preparing the graphs contained in this paper and for producing an in extenso version that contains detailed results from all computed cases and a printout of the computer program, as *Rand memorandum RM-6003-PR*, November 1969.

This research was made possible by continued support from the Office of Naval Research, Arctic Program, under contract N00014-67-A-0103-0007.

REFERENCES

Abels, G., Measurement of the snow density at Ekaterinburg during the winter of 1890–1891, *Acad. Nauk, Mem.*, *62*, 1–21, 1892.

Arnold, K. C., An investigation into methods of accelerating the melting of ice and snow by artificial dusting, in *Geology of the Arctic*, *2*, 989–1015, University of Toronto Press, 1961.

Badgley, F. I., Heat balance at the surface of the Arctic Ocean, *Proc. West. Snow Conf.*, 101–104, Spokane, Washington, 1961.

Barnes, H. T., *Ice Engineering*, 364 pp., Renouf, Montreal, 1928.

Bilello, M., Formation, growth and decay of sea ice in the Canadian Arctic Archipelago, *Arctic*, *14*, 2–25, 1961.

Bilello, M., Method for predicting river and lake ice formation, *J. Appl. Meteorol.*, *3*, 32–44, 1964.

Brooks, C. E. P., *Climate Through the Ages*, 395 pp., McGraw-Hill, New York, 1949.

Bryan, K., and M. D. Cox, A nonlinear model of an ocean driven by wind and differential heating, 1, Description of the three-dimension velocity and density fields, *J. Atmos. Sci.*, 2 945–967, 1968.

Budyko, M. I., Polar ice and climate, in *Proce ings of the Symposium on the Arctic He Budget and Atmospheric Circulation*, edited b J. O. Fletcher, pp. 3–22, The Rand Corporatio Santa Monica, California, RM-5233-NSF, 19

Chernigovskii, N. T., Radiational properties the Central Arctic ice cont, in *Soviet Data the Arctic Heat Budget and Its Climatic I fluence*, edited by J. O. Fletcher, J. Keller, a S. M. Olenicoff, pp. 151–174, The Rand Co poration, Santa Monica, California, RM-500 PR, 1966.

Coachman, L. K., Production of supercooled wat during sea ice formation, in *Proceedings of t Symposium on the Arctic Heat Budget a Atmospheric Circulation*, edited by J. Fletcher, pp. 497–529, The Rand Corporatio Santa Monica, California, RM-5233-NSF, 19

Crary, A. P., Arctic ice island and shelf ice studie in *Scientific Studies at Fletcher's Ice Island, T 1952–1958*, *3*, 1–37, GRD-AFCRC, *Geophys. Re Pap. 05*, 1960.

Doos, W. L., and M. Ewing, A theory of ice age 3, *Science*, *132*, 1706–1712, 1960.

Doos, W. L., and D. M. Shaw, The heat budg of an ice-free and an ice-covered Arctic Ocea *J. Geophysical Res.*, *71*, 1057–1063, 1966.

Doronin, Yu. P., On the problem of sea ice a cretion (in Russian), *Probl. Arkt. Antarkt.*, 73–80, 1959.

Doronin, Yu. P., On the heat balance of the Ce tral Arctic (in Russian), *Proc. Arctic Antarct Res. Inst.*, *268*, 178–184, 1963.

Doronin, Yu. P., Characteristics of the heat e change, in *Proceedings of the Symposium the Arctic Heat Budget and Atmospheric Ci culation*, edited by J. O. Fletcher, pp. 247–25 The Rand Corporation, Santa Monica, Califo nia, RM-5233-NSF, 1965.

Ewing, M., and W. L. Donn, A theory of i ages, 1, *Science*, *123*, 1061–1066, 1956.

Ewing, M., and W. L. Donn, A theory of ice ag 2, *Science*, *127*, 1159–1162, 1958.

Fletcher, J. O., *The Heat Budget of the Arct Basin and Its Relation to Climate*, 179 pp., T Rand Corporation, Santa Monica, Californi R-444-PR, 1965.

Fletcher, J. O., *Ice Extent on the Southern Ocea and Its Relation to World Climate*, 108 p The Rand Corporation, Santa Monica, Ca fornia, RM-5781-NSF, 1969.

Harrison, A. M., Studies of the mass budget arctic pack-ice floes, *J. Glaciol.*, *5*, 701–709, 19

Hisdal, V., The diurnal temperature variati during the polar night, *Quart. J. Roy. Meteor Soc.*, *86*, 104–106, 1960.

Kellogg, W. W., K. J. K. Buettner, and E. C. Ma *Meteorological Satellite Observations of The mal Emission*, 102 pp., The Rand Corporatio Santa Monica, California, RM-4392-NASA, 19

Kolesnikov, A. G., On the theory of ice accreti

on the sea surface (in Russian), in *Problems of Marine Hydrological Forecasts*, pp. 102–147, Leningrad, 1945.

Luktionov, A. F., Recent Soviet investigations in the polar regions, in *Sea Transport Publishing*, pp. 347–426 1935. (Translation by Air University Document Study, Maxwell AFB, 1950.)

Langleben, M. P., Albedo measurements on an arctic ice cover from high towers, *J. Glaciol.*, *7*, 283–293, 1968.

Larkin, B. K., Stable difference approximations to the diffusion equation, *Math. Comput.*, *18*, 196–202, 1964.

Lyon, W., *Ocean and Sea Ice Research in the Arctic Ocean*, Transl., New York Academy of Sciences, series 2, 23, 1961.

Malmgren, F., On the properties of sea ice, in *The Norwegian Polar Expedition 'Maud,' Scientific Results*, *1*c(5), 1–67, 1927.

Manabe, S., and K. Bryan, Climate calculations with a combined ocean-atmosphere model, *J. Atmos. Sci.*, *26*, 786–789, 1969.

Marshunova, M. S., Principal characteristics of the radiation balance of the underlying surface and of the atmosphere in the Arctic, *Proc. Arctic Antarctic Res. Inst.*, 239, 1961. (Translated by the Rand Corporation, RM-6003-PR, 1966.)

Maykut, G. A., and N. Untersteiner, *Numerical Prediction of the Thermodynamic Response of Arctic Sea Ice to Environmental Changes*, 173 pp., The Rand Corporation, RM-6093-PR, 1969.

Mosby, H., Water, salt, and heat balance in the North Polar Sea, *Proc. Arctic Basin Symp.*, pp. 69–84, Arctic Institute of North America, Washington, D. C., 1963.

Ono, N., Specific heat and heat of fusion of sea ice, in *Physics of Snow and Ice*, Volume I, edited by H. Oura, pp. 599–610, Institute of Low Temperature Science, Hokkaido, Japan, 1967.

Panov, V. V., and A. O. Shpaikher, Influence of Atlantic waters on some features of the hydrology of the Arctic Basin and adjacent seas, *Deep-Sea Res.*, *11*, 375–385, 1964.

Petrov, I. G., Physical-mechanical properties and thickness of the ice cover, in *Observational Data of the Scientific-Research Drifting Station of 1950–1951*, *3*(6), edited by M. M. Somov, 113 pp., 1964. (Translation for GRD by American Meteorological Society under contract AF(604)-1938.)

Richtmyer, R. D., *Difference Methods for Initial Value Problems*, 238 pp., Interscience, New York, 1957.

Saul'ev, V. K., A method of numerical solution for the diffusion equation (in Russian), *Dokl. Akad. Nauk SSSR(NS)*, *115*, 1077–1079, 1957a.

Saul'ev, V. K., Numerical integration of parabolic equations (in Russian), *Dokl. Akad. Nauk SSSR (NS)*, *117*, 26–30, 1957b.

Schwarzacher, W., Pack ice studies in the Arctic Ocean, *J. Geophys. Res.*, *64*, 2357–2367, 1959.

Schwerdtfeger, P., The thermal properties of sea ice, *J. Glaciol.*, *4*, 789–807, 1963.

Schwerdtfeger, P., An analogue computer for solving growth problems of floating ice, *Geofis. Pura Appl. Geofisica*, *75*, 44–52, 1964.

Stefan, J., Über die Theorie der Eisbildung, insbesondere über die Eisbildung im Polarmeer, *Ann. Physik, 3rd Ser.*, *42*, 269–286, 1891.

Tryakhov, L. C., Is it possible to remove the ice cover of the Northern Arctic Ocean?, *Priroda*, *11*, 93–97, 1963. (Translation for AFCRL, [illegible] Emmanuel College Research Language Center, E-T-R-64-23.)

U. S. Naval Civil Engineering Laboratory, *Theoretical Study of an Arctic Ocean Environment Simulator*, Port Hueneme, California, rep. 309, 189 pp., 1965.

Untersteiner, N., On the mass and heat budget of arctic sea ice, *Arch. Meteorol. Geophys. Biokl. Ser. A*, *12*, 151–182, 1961.

Untersteiner, N., Calculations of temperature regime and heat budget of sea ice in the Central Arctic, *J. Geophys. Res.*, *69*, 4755–4766, 1964.

Untersteiner, N., Calculating the thermal regime and mass budget of sea ice, in *Proceedings of the Symposium on the Arctic Heat Budget and Atmospheric Circulation*, edited by J. O. Fletcher, pp. 203–214, The Rand Corporation, Santa Monica, California, RM-5233-NSF, 1967.

Untersteiner, N., Natural desalination and equilibrium salinity profile of perennial sea ice, *J. Geophys. Res.*, *73*, 1251–1257, 1968.

Vowinckel, E., and S. Orvig, Energy balance of the Arctic, 5, The heat budget of the Arctic Ocean, *Arch. Meteorol. Geophys. Bioklimatol. A*, *14*, 303–326, 1966.

Vowinckel, E., and S. Orvig, Climate change over the Polar Ocean, I, The radiation budget, *Arch. Meteorol. Geophys. Bioklimatol., A*, *15*, 1–2, 1967.

Wittmann, W. I., and J. J. Schule, Comments on the mass budget of arctic pack ice, in *Proceedings of the Symposium on the Arctic Heat Budget and Atmospheric Circulation*, edited by J. O. Fletcher, pp. 215–246, The Rand Corporation, Santa Monica, California, RM-5233-NSF, 1966.

Yunes, A. V., Melting of snow and ice in the Central Arctic, in *Problems of the Arctic and the Antarctic, No. 11*, edited by A. F. Trashnikov, 91–93, Arctic and Antarctic Research Institute, Leningrad, 1962. (Translated for AINA, Mc 1966.)

Zubov, N. N., *Arctic Ice (Issledovaniya Okeana morpotil)*, 360 pp., Moscow, 1943. (Translated for AFCRC by U. S. Naval Oceanographic Office and American Meteorological Society.)

(Received September 9, 1970;
revised November 25, 1970.)